

AD-A021 588

EXPERIMENTAL DETERMINATION OF HYDRODYNAMIC LOADING
FOR TEN CABLE FAIRING MODELS

R, Folb

David W. Taylor Naval Ship REsearch and Development
Center
Bethesda, Maryland

November 1975

DISTRIBUTED BY:

NTIS

National Technical Information Service
U. S. DEPARTMENT OF COMMERCE

Report #310

**DAVID W. TAYLOR
NAVAL SHIP RESEARCH AND DEVELOPMENT CENTER**

Bethesda, Maryland 2084



ADA021588

**EXPERIMENTAL DETERMINATION OF HYDRODYNAMIC
LOADING FOR TEN CABLE FAIRING MODELS**

by

R. Folb

APPROVED FOR PUBLIC RELEASE: DISTRIBUTION UNLIMITED

SHIP PERFORMANCE DEPARTMENT
RESEARCH AND DEVELOPMENT REPORT

DDC
RECEIVED
MAR 16 1976
RECEIVED
C

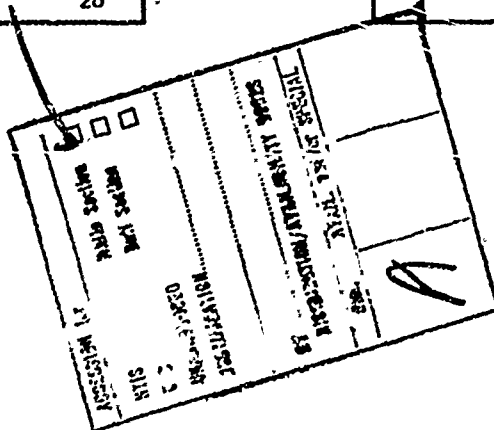
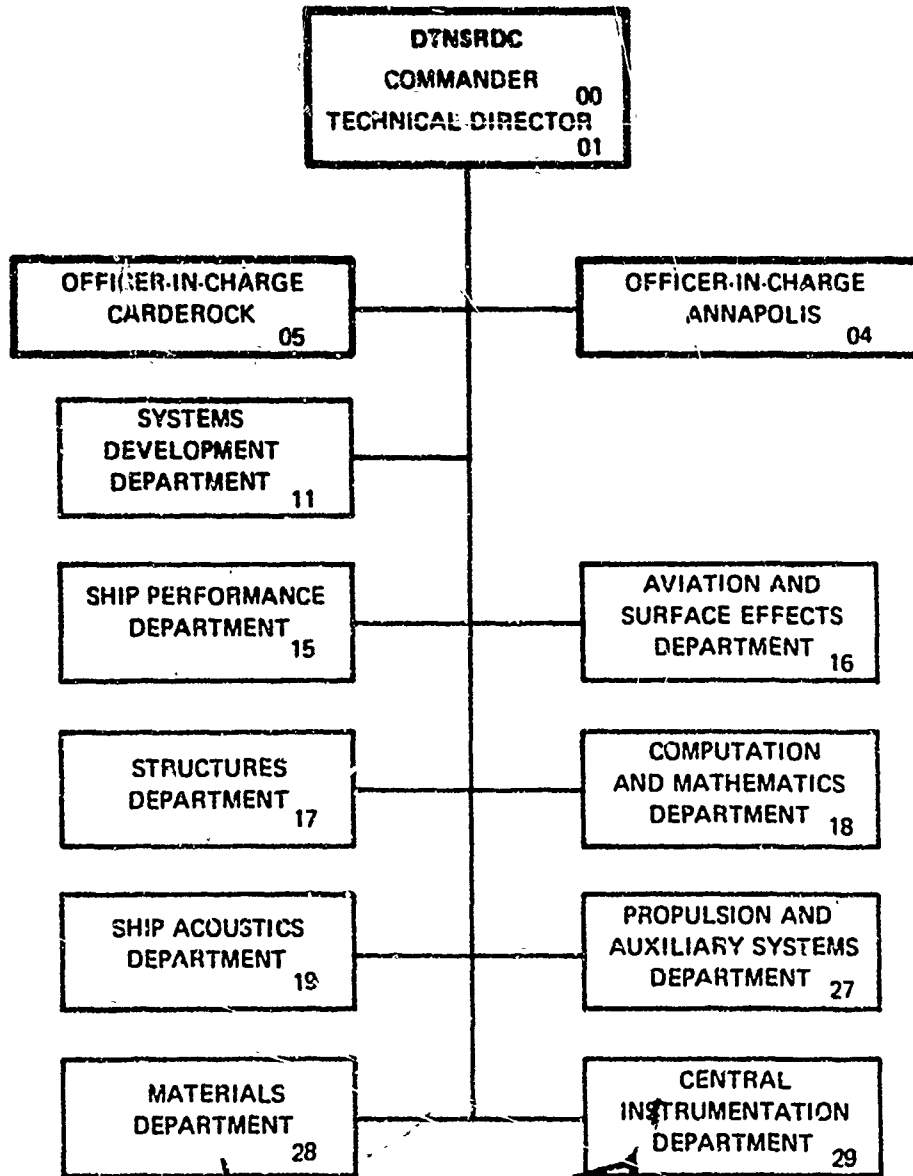
November 1975

Report 4810

Reproduced by
NATIONAL TECHNICAL
INFORMATION SERVICE
U.S. Department of Commerce
Springfield, MA 01115

EXPERIMENTAL DETERMINATION OF HYDRODYNAMIC LOADING FOR TEN CABLE FAIRING MODELS

MAJOR DTNSRDC ORGANIZATIONAL COMPONENTS



UNCLASSIFIED

SECURITY CLASSIFICATION OF THIS PAGE (When Data Entered)

REPORT DOCUMENTATION PAGE		READ INSTRUCTIONS BEFORE COMPLETING FORM
1 REPORT NUMBER 4610	2. GOVT ACCESSION NO.	3 RECIPIENT'S CATALOG NUMBER
4 TITLE (and Subtitle) EXPERIMENTAL DETERMINATION OF HYDRODYNAMIC LOADING FOR TEN CABLE FAIRING MODELS		5. TYPE OF REPORT & PERIOD COVERED
		6 PERFORMING ORG. REPORT NUMBER
7 AUTHOR(s) R. Folb		8 CONTRACT OR GRANT NUMBER(s)
9 PERFORMING ORGANIZATION NAME AND ADDRESS David W. Taylor Naval Ship Research and Development Center - Bethesda, Maryland 20084		10 PROGRAM ELEMENT, PROJECT, TASK AREA & WORK UNIT NUMBERS Program Element 62755N Task Area 2F54-544-001 Work Unit 1-1548-208
11 CONTROLLING OFFICE NAME AND ADDRESS David W. Taylor Naval Ship Research and Development Center - Bethesda, Maryland 20084		12. REPORT DATE November 1975
		13 NUMBER OF PAGES 79
14 MONITORING AGENCY NAME & ADDRESS (if different from Controlling Office)		15. SECURITY CLASS. (of this report) UNCLASSIFIED
		15a. DECLASSIFICATION/DOWNGRADING SCHEDULE
16 DISTRIBUTION STATEMENT (of this Report) APPROVED FOR PUBLIC RELEASE: DISTRIBUTION UNLIMITED		
17 DISTRIBUTION STATEMENT (of the abstract entered in Block 20, if different from Report)		
18 SUPPLEMENTARY NOTES		
19 KEY WORDS (Continue on reverse side if necessary and identify by block number) Cable Fairing Fairing Shapes Hydrodynamic Forces Fairing Tests Loading Functions Drag Coefficients		
20 ABSTRACT (Continue on reverse side if necessary and identify by block number) The David W. Taylor Naval Ship Research and Development Center has undertaken the measurement of the two-dimensional hydrodynamic loading on faired cable models as the first part of a program to improve towing configuration prediction capability. The experimental approach consists of measuring the normal and tangential hydrodynamic force components on (Continued on reverse side)		

UNCLASSIFIED

SECURITY CLASSIFICATION OF THIS PAGE(When Data Entered)

(Block 20 continued)

models towed in the high speed basin over a range of speeds, cable angles, and wetted lengths, using a special Cable Fairing Dynamometer. From these measurements the drag coefficients and hydrodynamic loading functions are obtained. To date, ten fairing models have been so characterized. The value of these loading functions to configuration prediction remains to be demonstrated by correlation with at-sea measurements.

UNCLASSIFIED

SECURITY CLASSIFICATION OF THIS PAGE(When Data Entered)

TABLE OF CONTENTS

	Page
ABSTRACT	1
ADMINISTRATIVE INFORMATION	1
INTRODUCTION	1
DESCRIPTIONS OF THE FAIRING MODELS	3
EXPERIMENTAL APPARATUS AND PROCEDURES	15
CABLE FAIRING DYNAMOMETER	15
TOWING GIRDER DYNAMOMETER	18
EXPERIMENTAL PROCEDURES	18
DATA ANALYSIS	18
HYDRODYNAMIC FORCES	22
HYDRODYNAMIC LOADING FUNCTIONS	24
DRAG COEFFICIENT	25
EXPERIMENTAL RESULTS	25
DISCUSSION	27
CONCLUSIONS	30
ACKNOWLEDGMENTS	30
APPENDIX A – TABULATED FORCE MEASUREMENT DATA	31
APPENDIX B – TABULATED VALUES OF THE HYDRODYNAMIC FORCES	41
APPENDIX C – TABULATED VALUES OF THE LOADING FUNCTIONS	49
APPENDIX D – GRAPHS OF THE HYDRODYNAMIC LOADING FUNCTIONS	55
APPENDIX E – GRAPHS OF DRAG COEFFICIENTS	67
REFERENCES	73

LIST OF FIGURES

	Page
1 – Model A Configured for the Towing Girder Dynamometer	6
2 – Model B, Components of a Section	6
3 – Model C	8
4 – Close Up View of Model C	8
5 – Close Up View of Model D	8
6 – Model E	10
7 – Model F	10
8 – Analytic Function of Section Dimensional Offsets for Models F, G, and H	11
9 – Model G	12
10 – Model H	12
11 – Model I	14
12 – Ribbon Cable Model J	14
13 – Cable Fairing Dynamometer with Model Attached	16
14 – Force Coordinate System	17
15 – Schematic Arrangement of Towing Girder Dynamometer	19
16 – Typical Curves of Hydrodynamic Force versus Wetted Length	23
17 – Drag Coefficient versus Reynolds Number	29
D.1 – Normal Loading Function f_n versus Cable Angle for Model A	56
D.2 – Tangential Loading Function f_t versus Cable Angle for Model A	56
D.3 – Normal Loading Function f_n versus Cable Angle for Model B	57
D.4 – Tangential Loading Function f_t versus Cable Angle for Model B	57
D.5 – Normal Loading Function f_n versus Cable Angle for Model C	58
D.6 – Tangential Loading Function f_t versus Cable Angle for Model C	58

	Page
D. 7 – Normal Loading Function f_n versus Cable Angle for Model D	59
D. 8 – Tangential Loading Function f_t versus Cable Angle for Model D	59
D. 9 – Normal Loading Function f_n versus Cable Angle for Model E	60
D.10 – Tangential Loading Function f_t versus Cable Angle for Model E	60
D.11 – Normal Loading Function f_n versus Cable Angle for Model F	61
D.12 – Tangential Loading Function f_t versus Cable Angle for Model F	61
D.13 – Normal Loading Function f_n versus Cable Angle for Model G	62
D.14 – Tangential Loading Function f_t versus Cable Angle for Model G	62
D.15 – Normal Loading Function f_n versus Cable Angle for Model H	63
D.16 – Tangential Loading Function f_t versus Cable Angle for Model H	63
D.17 – Normal Loading Function f_n versus Cable Angle for Model I	64
D.18 – Tangential Loading Function f_t versus Cable Angle for Model I	64
D.19 – Normal Loading Function f_n versus Cable Angle for Model J	65
D.20 – Tangential Loading Function f_t versus Cable Angle for Model J	65
E.1 – Drag Coefficient versus Reynolds Number for Model A	68
E.2 – Drag Coefficient versus Reynolds Number for Model B	68
E.3 – Drag Coefficient versus Reynolds Number for Model C	69
E.4 – Drag Coefficient versus Reynolds Number for Model D	69
E.5 – Drag Coefficient versus Reynolds Number for Model E	70
E.6 – Drag Coefficient versus Reynolds Number for Model F	70

	Page
E. 7 - Drag Coefficient versus Reynolds Number for Model G	71
E. 8 - Drag Coefficient versus Reynolds Number for Model H	71
E. 9 - Drag Coefficient versus Reynolds Number for Model I	72
E.10 - Drag Coefficient versus Reynolds Number for Model J	72

LIST OF TABLES

1 - Physical Characteristics of Fairing Models	4
2 - Dimensional Offsets for Fairing Model A	5
3 - Dimensional Offsets for Fairing Models B, C, and D	5
4 - Dimensional Offsets for Fairing Model E	9
5 - Dimensional Offsets for Fairing Model F	9
6 - Dimensional Offsets for Fairing Models G and H	13
7 - Dimensional Offsets for Fairing Model I	13
8 - Angles of Inclination	20
9 - Wetted Length	20
10 - Speed Range	21
11 - Boundary Conditions for Analytic Functions	26
12 - Hydrodynamic Loading Function Coefficients	28
A.1 - Experimental Data for the Faired-Cable Model G	32
B.1 - Two-Dimensional Hydrodynamic Forces on Model A	42
B.2 - Two-Dimensional Hydrodynamic Forces on Model B	42
B.3 - Two-Dimensional Hydrodynamic Forces on Model C	43
B.4 - Two-Dimensional Hydrodynamic Forces on Model D	43
B.5 - Two-Dimensional Hydrodynamic Forces on Model E	44
B.6 - Two-Dimensional Hydrodynamic Forces on Model I	46
C.1 - Values of Normalized Normal and Tangential Loading Function for Model B	50

	Page
C.2 – Values of Normalized Normal and Tangential Loading Function for Model E	51
C.3 – Values of Normalized Normal and Tangential Loading Function for Model F	52
C.4 – Values of Normalized Normal and Tangential Loading Function for Model H	52
C.5 – Values of Normalized Normal and Tangential Loading Function for Model I	53
C.6 – Values of Normalized Normal and Tangential Loading Function for Model J	54

NOTATION

A_n	Coefficient of $\cos n\phi$ terms in hydrodynamic loading function
A_0	Constant coefficient in hydrodynamic loading function
B_n	Coefficient of $\sin n\phi$ terms in hydrodynamic loading function
C_R	Cable fairing drag coefficient
c	Fairing chord length
d	Cable diameter
F_n, F_t	Hydrodynamic forces per unit length in the normal and tangential directions
f_n, f_t	Hydrodynamic loading functions in the normal and tangential directions
R	Drag per unit length of fairing when the fairing is normal to the free stream
R_n	Reynolds number
r	Radius
s	Fairing model wetted length
t	Maximum fairing thickness
V	Free stream velocity
X, Y, Z	Hydrodynamic forces in the normal, side and tangential directions
ν	Kinematic viscosity of fluid
ρ	Mass density of fluid
ϕ	Cable angle (acute angle between Z force direction and direction of motion)

ABSTRACT

The David W. Taylor Naval Ship Research and Development Center has undertaken the measurement of the two-dimensional hydrodynamic loading on faired cable models as the first part of a program to improve towing configuration prediction capability. The experimental approach consists of measuring the normal and tangential hydrodynamic force components on models towed in the high speed basin over a range of speeds, cable angles, and wetted lengths, using a special Cable Fairing Dynamometer. From these measurements the drag coefficients and hydrodynamic loading functions are obtained. To date, ten fairing models have been so characterized. The value of these loading functions to configuration prediction remains to be demonstrated by correlation with at-sea measurements.

ADMINISTRATIVE INFORMATION

The work described in this report was performed in support of a number of specific projects sponsored by the Naval Sea Systems Command, the Naval Ship Engineering Center and the Naval Air Systems Command. This composite report was funded by the Naval Material Command, under the Direct Laboratory Funding Program of Advanced Towline Technology Development, Program Element Number 62755N, Task Area Number ZF54-544-C01, David W. Taylor Naval Ship Research and Development Center Work Unit 1-1548-208.

INTRODUCTION

The David W. Taylor Naval Ship Research and Development Center is engaged in a research program to improve the analytical techniques used in predicting the steady-state towing configuration of cable-body systems. While the configuration represents in general a three-dimensional problem, program emphasis is currently on the two-dimensional case, i.e., the configuration in the plane defined by gravity and the free-stream velocity. The differential equations describing the two-dimensional equilibrium configuration resulting from the forces acting on the cable-body system were derived a number of years ago.¹ Solutions to these equations can be obtained numerically using a digital computer² provided the hydrodynamic forces on the body and the towline are known. The hydrodynamic forces acting on the towed

¹Pode, L., "Tables for Computing the Equilibrium Configuration of a Flexible Cable in a Uniform Stream," David Taylor Model Basin Report 687 (Mar 1951). A complete listing of references is given on page 73.

²Cuthill, E.H., "A FORTRAN IV Program for the Calculation of the Equilibrium Configuration of a Flexible Cable in a Uniform Stream," NSRDC Report 2531 (Feb 1958).

body can be calculated or obtained experimentally by established techniques. However, towline hydrodynamic loading is not generally known. Past practice at the Center has been to compute the towline configuration using the normal drag coefficient of the towline and one or another form of the hydrodynamic loading functions proposed by different investigators.^{1,3-5}

In dimensional form the hydrodynamic loading is expressed mathematically in terms of the hydrodynamic force components per unit length acting on an element of towline in the directions normal (F_n) and tangential (F_t) to its longitudinal axis. The principle of independence is assumed, i.e., the hydrodynamic force component per unit length acting on an element of a particular towline is dependent only on speed and the angle of inclination of the element to the free stream velocity.

The differential equations describing the two-dimensional equilibrium configuration generally accept as inputs the hydrodynamic loading expressions in normalized form. It has, therefore, become the convention to normalize F_n and F_t by the normal drag per unit length, R . In this normalized form the expressions are referred to as "the hydrodynamic loading functions."

Evaluating these functions for particular tows has been difficult, especially for faired tow cables which have wide variation in physical characteristics. The Center has initiated a three part program aimed at establishing an effective technique for determining the hydrodynamic loading functions for faired tow cables. The first element entails measuring the hydrodynamic loading on short sections of cable fairing models in the towing basin. The second is concerned with developing the methods of measuring at sea both the towing configuration and the hydrodynamic loading on real faired tow cables. Finally, correlation of the basin measurements with the at-sea measurements is required to verify the towing basin technique as a viable and effective method of obtaining the loading functions useful in predicting towing configurations.

The first part of the program has been ongoing since 1960. The experimental approach consists of towing rigid models of faired cable in the towing basin over a range of speeds, angles of inclination and wetted lengths, and measuring the hydrodynamic forces using the DTMB Cable-Fairing Dynamometer, developed specifically for this purpose. These force measurements are converted to drag coefficients and analytical expressions for the hydrodynamic loading functions. To date, ten different fairing models have been so characterized by different

³Whicker, L.F., "The Oscillatory Motion of Cable-Towed Bodies," University of California Report Series No. 82, Issue No. 2 (May 1957).

⁴Landweber, L. and M.H. Protter, "The Shape and Tension of a Light, Flexible Cable in a Uniform Current," David Taylor Model Basin Report 533 (Oct 1944).

⁵Fames, M.C., "Steady-State Theory of Towing Cables," Defence Research Establishment Atlantic Report 67/5 (1967).

investigations at the Center and the results reported informally. This report presents a compilation of the data obtained in the individual experiments. The report includes descriptions of the ten models, the towing dynamometers, the experimental procedures, and the data reduction techniques. The experimental results are presented as analytical expressions of the normal and tangential hydrodynamic loading functions and graphs of the drag coefficients versus Reynolds number for each fairing model.

The second and third elements of the program remain to be accomplished.

DESCRIPTIONS OF THE FAIRING MODELS

The ten fairing models tested have been designated alphabetically in this report as Model A through Model J. Fairing model physical characteristics are given in Table 1.

Model A has the characteristics of an enclosed, continuous fairing with the section shape of TMB Number 7. The equations used to develop the dimensional offsets are given in Reference 6 and the offsets given in Table 2. The model consists of a five-segment aluminum strut which can be configured for both the cable fairing and towing girder dynamometers. Figure 1 shows Model A configured for the towing girder dynamometer. When so configured, model length is varied by adding short segments to the strut. Nose and tail fairings are also used for streamlining.

Model B also has the cross-sectional shape of TMB Number 7, but it has the characteristics of an enclosed, sectional fairing similar to that in use on the AN/SQA-10 Variable Depth Sonar system. The offsets are given in Table 3. The model consists of a simulated cable element on which ten sections of fairing are attached. A typical section, shown in Figure 2, is composed of a hard plastic afterbody, a stainless steel headpiece, alignment rods and associated hardware. The completed model forms an enclosed fairing model with a scalloped leading edge provided to meet the requirement for drum storage. The simulated cable, 2.4 inches in diameter, consists of twenty-four 0.25-inch-diameter copper strands with left-hand lay, joined to a seamless tube.

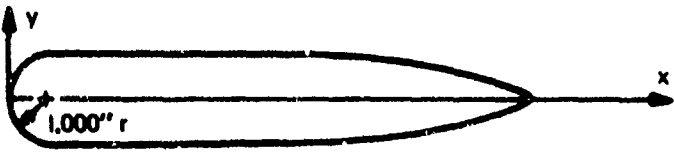
Model C is a model of an enclosed, sectional fairing having the TMB Number 7 shape, but in which the discontinuities between adjacent afterbody sections have been eliminated. It consists of a simulated stranded cable element on which ten headpieces of standard sectional fairing are attached. The trailing edge (after portion) is composed of a single piece of wood.

⁶Felhner, L.F. and L. Pode., "The Development of a Fairing for Tow Cables," David Taylor Model Basin Report C-433 (Jan 1952) UNCLASSIFIED.

TABLE 1 - PHYSICAL CHARACTERISTICS OF FAIRING MODELS

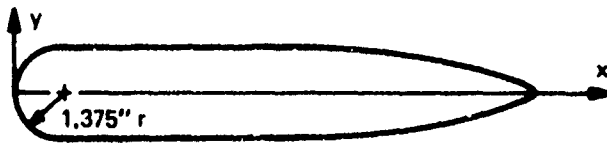
Characteristics	Fairing Models									
	A	B	C	D	E	F	G	H	I	J
Model Length, inches	89.25	84.0	84.0	84.0	89.25	89.25	88.8	89.2	84.0	85.0
Chord, inches	12.0	16.5	16.5	16.5	10.6	7.75	6.91	6.91	13.25	N/A
Maximum Fairing Thickness, inches	2.00	2.75	2.75	2.75	1.67	1.60	1.37	1.37	2.92	N/A
Cable Diameter, inches	N/A	2.40	2.40	2.40	2.00	2.00	2.00	2.00	N/A	2.00
Section Height, inches	N/A	8.25	8.25	8.25	N/A	N/A	N/A	N/A	N/A	N/A
Projected Frontal Area, square feet	1.24	1.60	1.60	1.60	1.24	1.24	1.23	1.24	1.7	N/A
Wetted Surface Area, square feet	15.83	20.42	20.42	20.42	14.25	10.6	9.35	9.41	15.46	N/A
Distance Between Cable and Fairing, inches	N/A	N/A	N/A	N/A	0.186	0	0	0	N/A	N/A
Clip Diameter, inches	N/A	N/A	N/A	N/A	N/A	N/A	0.50	N/A	N/A	N/A
Clip Width, inches	N/A	N/A	N/A	N/A	1.50	0.74	N/A	2.16	N/A	N/A
Clip Thickness, inches	N/A	N/A	N/A	N/A	0.09	0.04	N/A	0.19	N/A	N/A
Clip Spacing (Approximate), inches	N/A	N/A	N/A	N/A	10.0	12.0	11.4	11.4	N/A	N/A
Ribbon Loop Length, inches	N/A	N/A	N/A	N/A	N/A	N/A	N/A	N/A	N/A	37.0
Ribbon Width, inches	N/A	N/A	N/A	N/A	N/A	N/A	N/A	N/A	N/A	2.75
Ribbon Thickness, inches	N/A	N/A	N/A	N/A	N/A	N/A	N/A	N/A	N/A	0.0625
Vertical Ribbon Spacing, inches	N/A	N/A	N/A	N/A	N/A	N/A	N/A	N/A	N/A	0.4060
Ribbon Angle, θ , degrees	N/A	N/A	N/A	N/A	N/A	N/A	N/A	N/A	N/A	22.5
Model Length for Towing Girder, inches	113.25 89.25	N/A	N/A	N/A	N/A	N/A	N/A	N/A	N/A	N/A

TABLE 2 – DIMENSIONAL OFFSETS FOR FAIRING MODEL A



x IN INCHES	±y IN INCHES
1.000	1.000
2.000	1.000
3.000	1.000
4.000	1.000
5.000	0.999
6.000	0.998
7.000	0.959
8.000	0.902
9.000	0.809
10.000	0.670
11.000	0.474
11.500	0.335
12.000	0.000

TABLE 3 – DIMENSIONAL OFFSETS FOR FAIRING MODELS B, C, AND D



x IN INCHES	±y IN INCHES
1.375	1.375
2.000	1.375
4.000	1.375
7.000	1.372
8.000	1.362
9.000	1.340
10.000	1.302
11.000	1.241
12.000	1.153
13.000	1.035
14.000	0.879
15.000	0.681
15.750	0.482
16.000	0.393
16.500	0.000



Figure 1 – Model A Configured for the Towing Girder Dynamometer

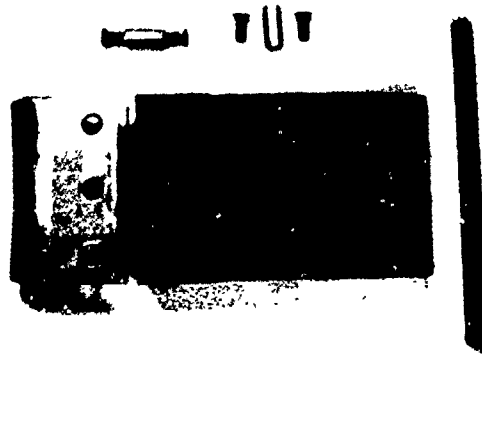


Figure 2 – Model B, Components of a Section

Each headpiece is placed over the simulated cable and attached to the continuous tail piece forming a 7-foot long model, shown in Figure 3. The assembly forms an enclosed fairing model with a gapped and a scalloped leading edge to accommodate drum storage.

Model D is the same as Model C except that the gaps in the leading edge are closed. The difference between Models C and D can be seen by comparing Figures 4 and 5.

Model E has the characteristics of a continuous, trailing fairing. Its section shape is a modified TMB Number 7. The dimensional offsets are given in Table 4. The model consists of a simulated stranded cable and the trailing fairing attached by equally spaced clips as shown in Figure 6. The cable element consists of twenty-four 0.219-inch-diameter strands with a 16.45-inch left-hand lay joined to a seamless steel tube.

Model F has characteristics of a continuous, trailing fairing attached to a simulated stranded cable by seven equally spaced clips as shown in Figure 7. The simulated cable is the same design used in the Model E experiments. The section dimensional offsets are generated by the equation given in Figure 8, using the parametric values listed in Table 1, except for the chord dimension. The shape was actually generated for a chord length of 8.0 inches. However, the fairing model was installed on the cable with no gap between the cable and fairing, resulting in an actual chord length of 7.75 inches. The offsets are given in Table 5.

Model G has the characteristics of a continuous, trailing fairing joined to a simulated stranded-cable element by eight equally-spaced clips as shown in Figure 9. The simulated cable is the same design used in the Model E experiments. The section dimensional offsets are generated by the equation in Figure 8 for a fairing thickness of 1.37 inches, a cable diameter of 1.715 inches and a chord of 6.86 inches. However, as with Model F, the fairing was installed on the 2-inch cable with no gap between cable and fairing. Because of the larger (2 inch) cable diameter, this resulted in an increase in chord length from the design value of 6.86 inches to the actual value of 6.91 inches. The offsets are given in Table 6. Model H, shown in Figure 10, is essentially the same as Model G except for differences in fairing clip design, as noted in Table 1.

Model I, shown in Figure 11, is a laminated mahogany strut having a modified NACA 63A022 section shape. The dimensional offsets are presented in Table 7.

Model J, shown in Figure 12, is a ribbon cable model composed of a simulated stranded cable element, a ribbon adapter and 27 ribbon loops. The ribbons were fabricated from rubber. The simulated cable is the same design used in the Model E experiments.

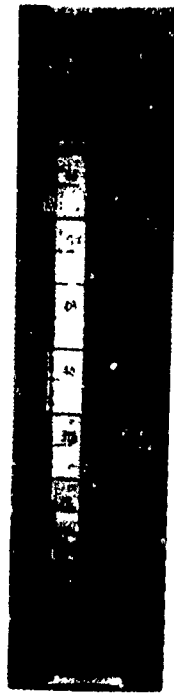


Figure 3 - Model C

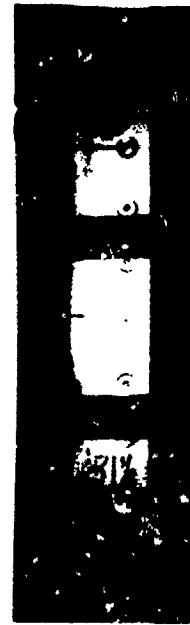


Figure 5 - Close Up View of Model D



Figure 4 - Close Up View of Model C

TABLE 4 – DIMENSIONAL OFFSETS FOR FAIRING MODEL E

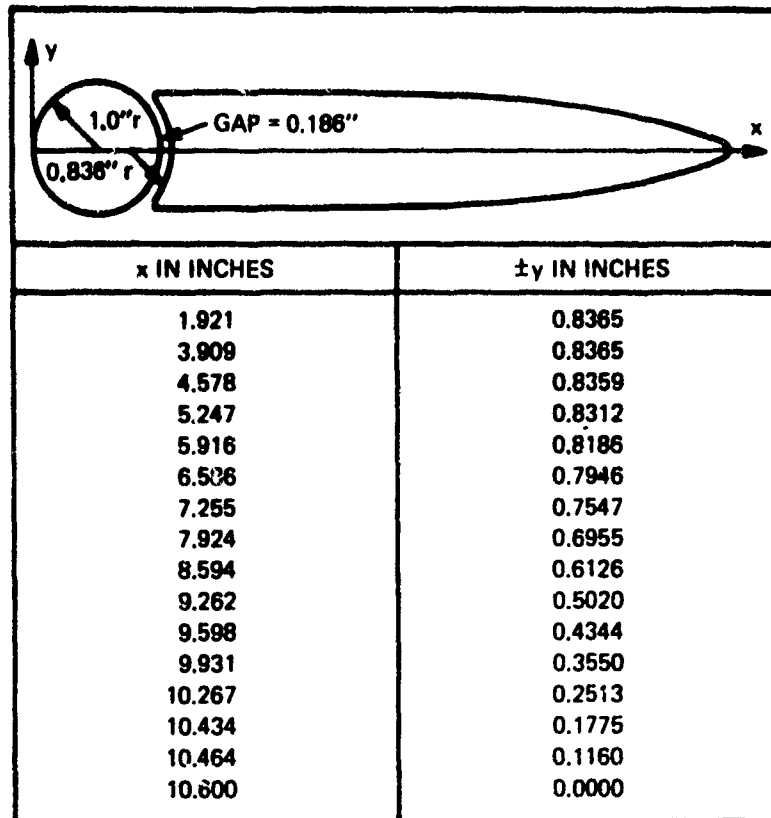


TABLE 5 – DIMENSIONAL OFFSETS FOR FAIRING MODEL F

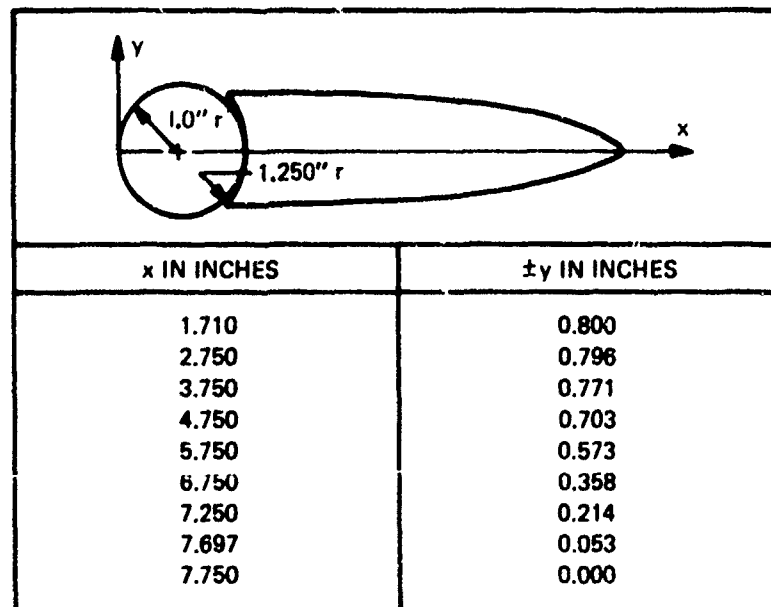


Figure 6 - Model E



SIMULATED CABLE

TRAILING FAIRING

FAIRING CLIPS

Figure 7 - Model F



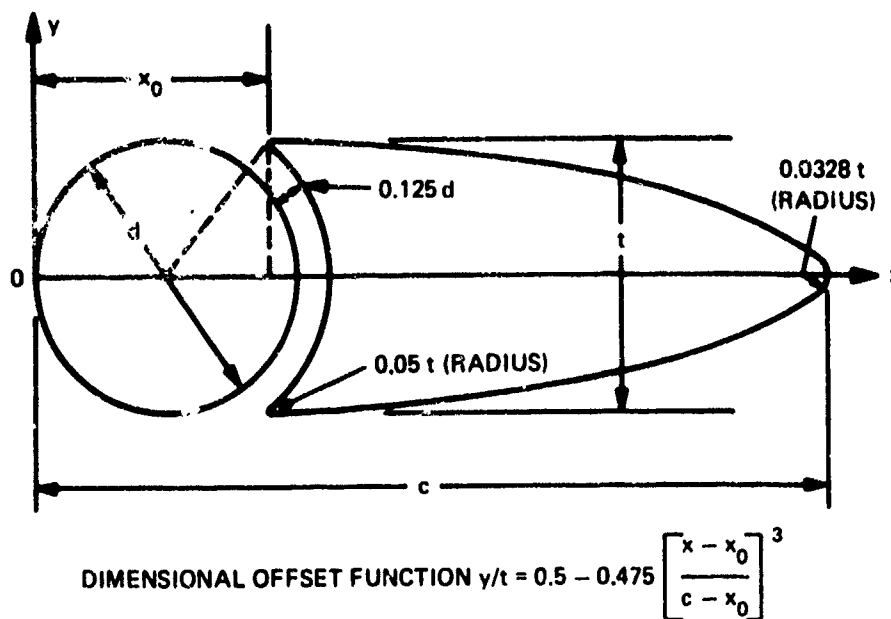


Figure 8 – Analytic Function of Section Dimensional Offsets for Models F, G, and H

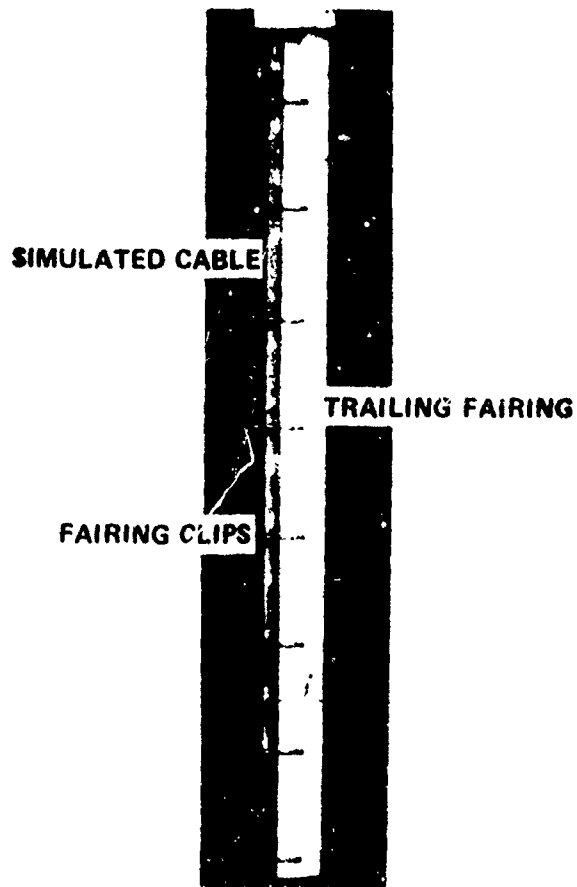


Figure 9 - Model G

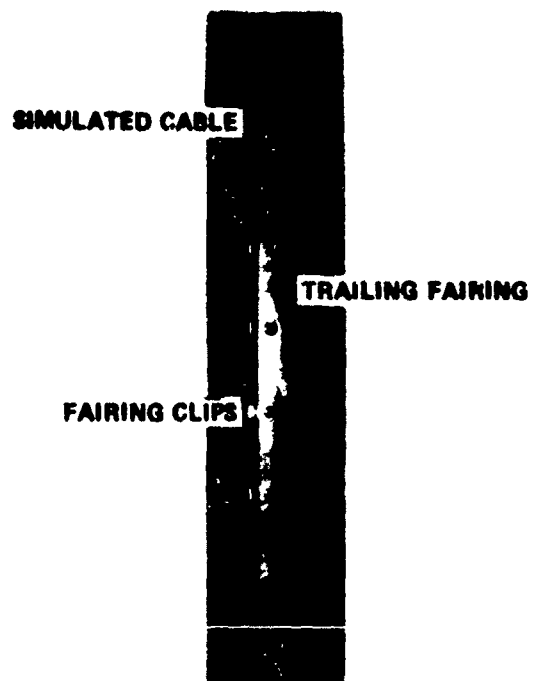
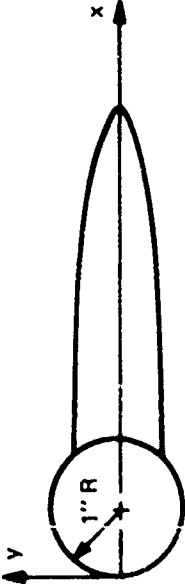



Figure 10 - Model H

TABLE 6 - DIMENSIONAL OFFSETS
FOR FAIRING MODELS G AND H



x IN INCHES	±y IN INCHES
1.750	0.685
2.050	0.685
3.050	0.674
4.050	0.627
5.050	0.514
6.050	0.308
6.550	0.161
6.865	0.045 RADIUS
6.910	0.000

TABLE 7 - DIMENSIONAL OFFSETS FOR FAIRING MODEL I



x IN INCHES	±y IN INCHES
0.0000	0.0000
0.0663	0.2337
0.0994	0.2814
0.1656	0.3583
0.3313	0.5011
0.6625	0.7030
0.9938	0.8516
1.3250	0.9711
1.9875	1.1546
2.6500	1.2862
3.3125	1.3780
3.9750	1.4348
4.6375	1.4567
5.3000	1.4448
5.9625	1.4021
6.6250	1.3327
7.2875	1.2411
7.9500	1.1310
8.6125	1.0053
9.2750	0.8683
9.9375	0.7250
10.6000	0.5813
11.2625	0.4376
11.9250	0.2938
12.5875	0.1500
13.2500	0.0062

LEADING EDGE RADIUS = 0.4645"
TRAILING EDGE RADIUS = 0.0106"

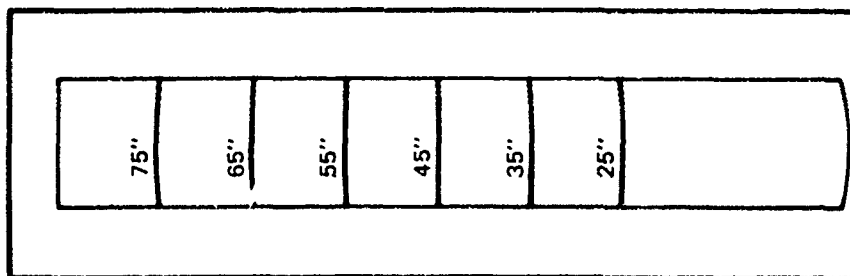


Figure 11 - Model I

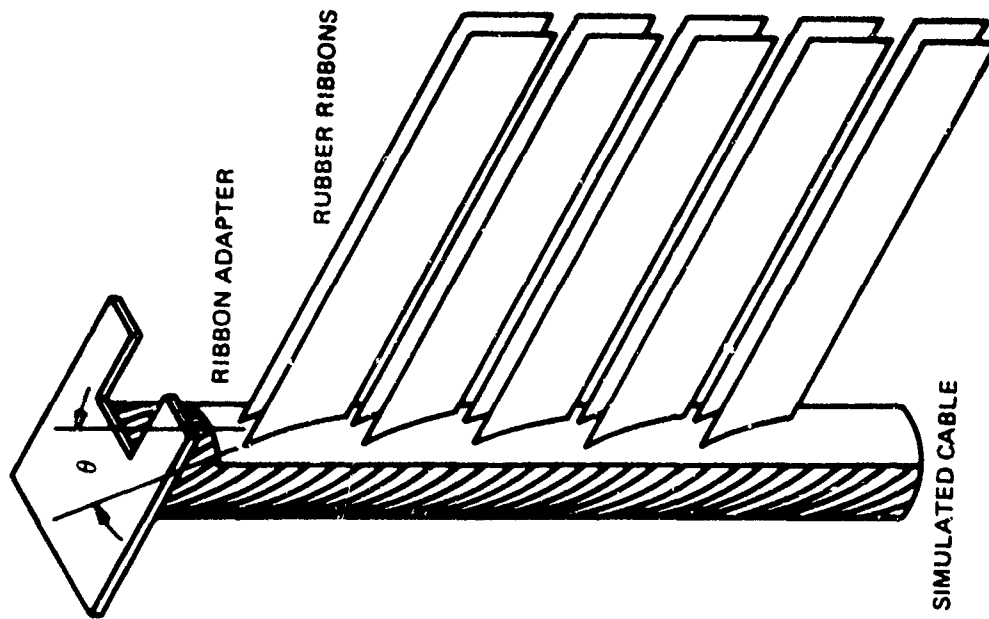


Figure 12 - Ribbon Cable Model J

EXPERIMENTAL APPARATUS AND PROCEDURES

The models were towed in the high-speed basin at the Center. A cable fairing dynamometer designed specifically for these experiments was used to measure the hydrodynamic forces. Model A, however, also was towed from the towing girder dynamometer to obtain hydrodynamic loading data at an angle of $\phi = 0$ deg (i.e., cable oriented parallel to the direction of flow). The dynamometers and experimental procedures are described in the following sections.

CABLE FAIRING DYNAMOMETER

The cable fairing dynamometer is shown in Figure 13 with the faired-cable Model C attached. The normal force X, side force Y, and tangential force Z acting on the model, as shown in Figure 14, are sensed by three 4-inch-cube modular force gages of the type described in Reference 7. Interchangeable force gages with capacities ranging from 50 to 1000 pounds are available. The dynamometer structural design, however, limits any of the three component forces to 500 pounds or less.

The tilt-table is adjustable so that the cable angle ϕ relative to the free stream may be varied from 90 to 30 degrees in 5-degree increments. The vertical position of the model and tilt-table is also adjustable by means of an electric hoist so that the model submergence may be varied from 0 to 7 feet. A weight-pan system provides a means of counterbalancing the model weight on the gages at each submergence and cable angle.

Instrumentation for these experiments consisted of the X force gage, selected from within a range between 50 and 500 pounds, a 1000-pound-capacity gage for the Y force, and a 50-pound-capacity gage for the Z force; two integrating digital voltmeters, a scanner and a printer for processing the X and Z gage signals; and a strip chart recorder for monitoring the Y force. Carriage speed was measured using a photo-cell and gear wheel with the signal input to an electronic counter. The estimated accuracy of the force measurement is approximately ± 0.5 percent of the rated full scale value of the particular gage used. The accuracy of the speed measurement is ± 0.05 knot.

⁷Gentler, M., "The DTMB Planar-Motion-Mechanism System," David Taylor Model Basin Report 2523 (Jul 1967).

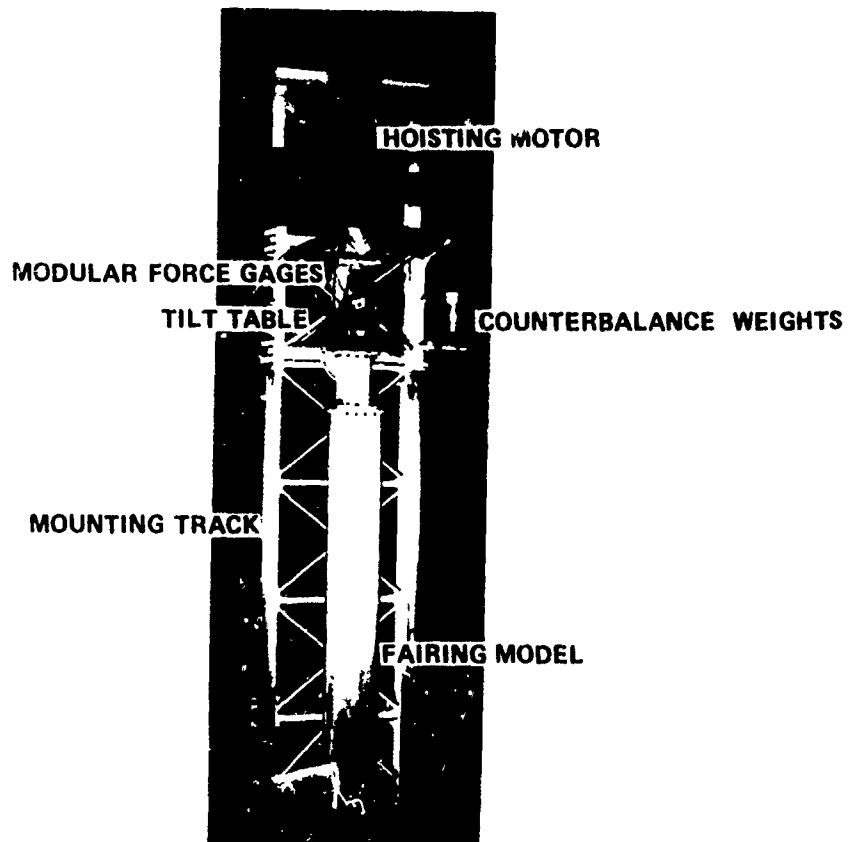


Figure 13 - Cable Fairing Dynamometer with Model Attached

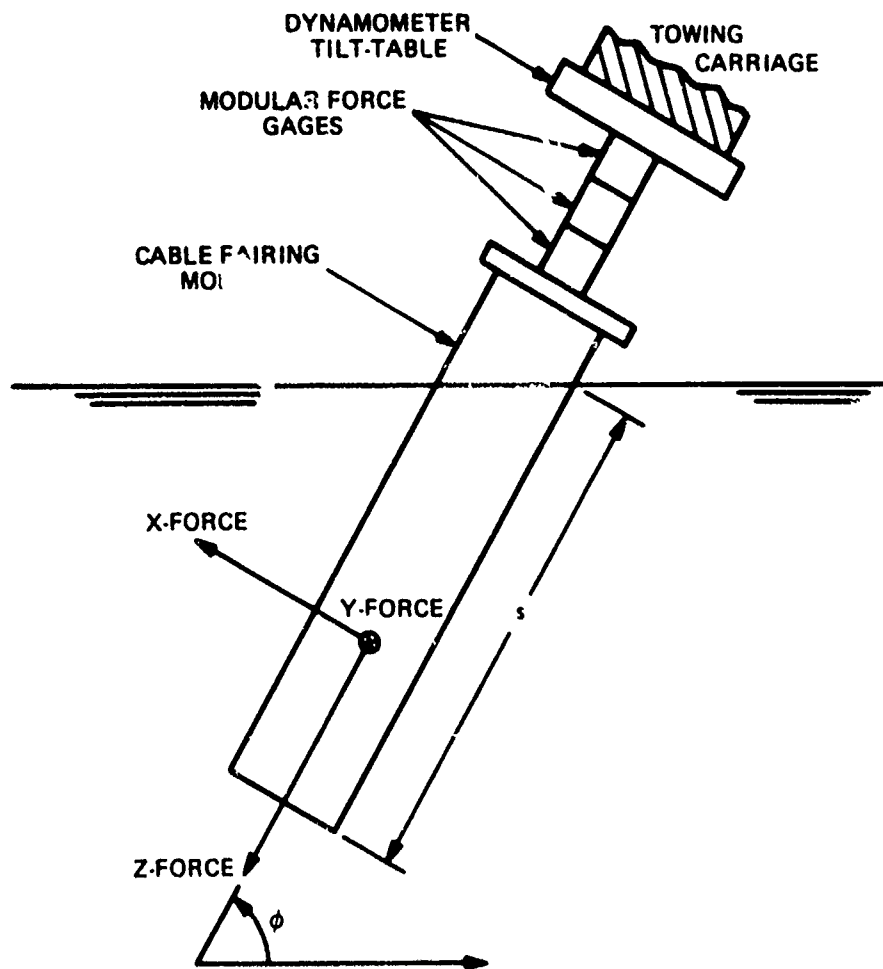


Figure 14 - Force Coordinate System

TOWING GIRDER DYNAMOMETER

The towing girder dynamometer used for the additional experiments on Model A is of the floating-frame weighing type and is illustrated diagrammatically in Figure 15. The dynamometer girder carries a long horizontal floating beam in pendulum fashion on two pairs of vertical arms terminating in flexible springs. A counterweight at the upper end of a vertical swinging arm mounted on the girder and attached to the floating beam maintains the beam in equilibrium at any position between the limit stops. The model resistance is transmitted as a horizontal force through the upper flexible link to the T-shaped balance, where it is balanced by weight. When the model resistance is not equal exactly to a unit weight, the difference is taken up by the resiliency of the flexible spring supports, the exact amount being recorded on the drum through the lower link and recording arm shown. A variable strength electro-magnetic dampener is incorporated to minimize model surge motions.

EXPERIMENTAL PROCEDURES

All ten models were towed in the high speed basin on the cable fairing dynamometer. Each model was towed at the angle of inclination to the flow indicated in Table 8. The model wetted length was varied over the range given in Table 9 for each angle. Each of the angle/wetted length combinations was towed at the speeds indicated in Table 10. For the special case of $\phi = 90$ deg, some of the models were towed at the additional speeds also noted in Table 10. Model A also was towed on the towing girder dynamometer in the deep water basin to obtain additional data at the angle $\phi = 0$ deg. As configured for the cable fairing dynamometer, Model A is referred to in Tables 8 through 10 as A(1); and for the floating girder dynamometer as A(2). The X and Z forces were recorded for each condition. The Y force was monitored to assist in aligning the model with the flow and to provide a means of observing lateral force oscillations.

DATA ANALYSIS

The measured data are first processed to obtain the two-dimensional hydrodynamic force components per unit length for each model. These values when normalized by R represent the normal and tangential hydrodynamic loading functions, f_n and f_t . The loading function values finally are processed to provide an analytic representation of the functions in the form of a trigonometric series. The drag coefficient C_R then is derived from the normal loading

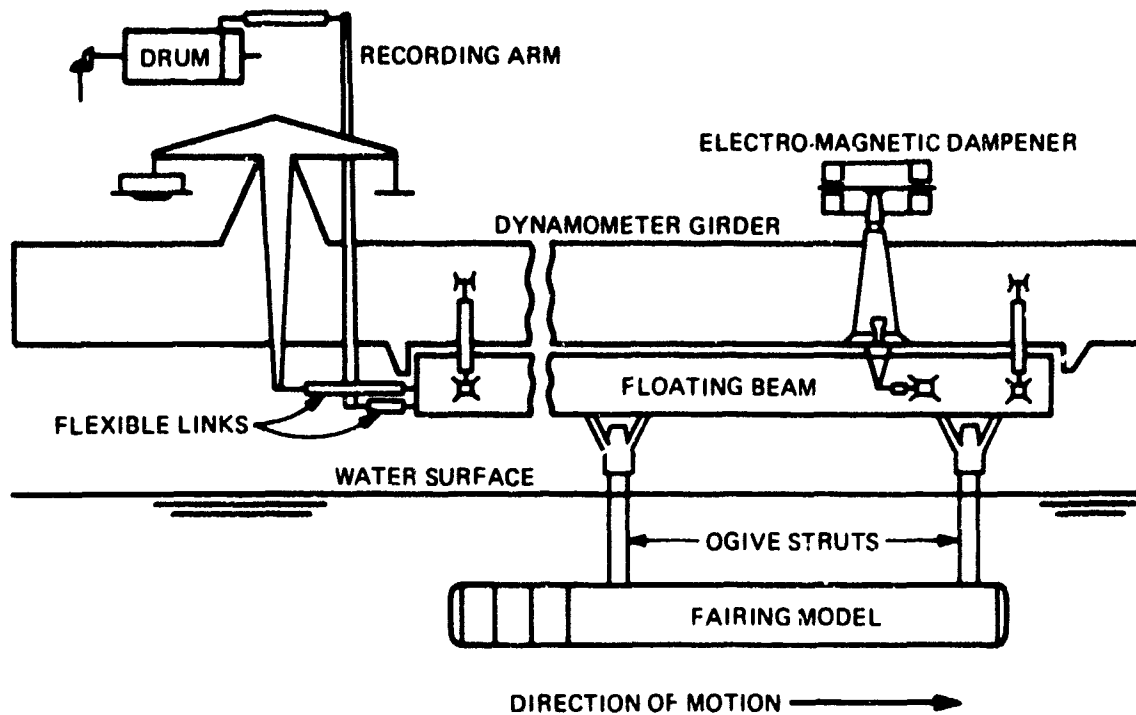


Figure 15 – Schematic Arrangement of Towing Girder Dynamometer

TABLE 8 – ANGLES OF INCLINATION

Model	Angles of Inclination ϕ , degrees
A(2)	0
B, G, H, A(1), J	From 90 to 30 in 10° increments
C	89.7, 84.9, 79.8, 74.9, 70.0, 60.2, 50.4, 40.5, 30.6
D	89.7, 69.7, 50.7, 40.3, 30.3
E, F	From 90 to 30 in 5° increments
I	89.9, 84.8, 79.8, 74.9, 68.8, 59.9, 49.8, 44.8, 39.9, 34.8, 29.9

TABLE 9 – WETTED LENGTH

Model	Wetted Length s , inches	Increment, inches
A(1)	24 to 84	6
A(2)	89.25 to 113.25	6
B	31 to 73.5	9
C, D	31.5 to 73.5	9
E	27 to 67	10
F	32 to 80	12
G	19 to 85	11
H	42 to 85	11
I	25 to 65	10
J	25 to 62	12.33

TABLE 10 - SPEED RANGE

Model	Speed, knots (All ϕ , All s)	Additional Speeds, knots ($\phi = 90^\circ$, All s)
A(1)	5, 8	2, 3, 4, 6, 8, 10, 13
A(2)	5, 8, 13	
B	2, 4, 6	1.0 to 10 in 1.0 increments
C, D	2, 4, 6, 8	
E	2.5, 3.5, 5.5, 6.5	1.0 to 7.0 in 0.5 increments
F	2, 4, 6, 8	0.75, 1.0, 1.5, 3, 5, 7
G	5, 8	0.8 to 5.0 in 0.5 increments
H	4, 5	
I	2, 4, 6, 8, 10	2.0 to 10.0 in 1.0 increments
J	5, 6, 7, 8	1.0, 2.0, 3.0

function evaluated at $\phi = 90$ deg and expressed as a function of Reynolds number. The following sections discuss the detailed methods of data reduction.

HYDRODYNAMIC FORCES

The determination of the components of hydrodynamic force per unit length is an intermediate step in developing loading functions. In that the models tested have relatively small aspect ratios and are surface piercing in these experiments, it is necessary to eliminate end effects from the force measurements to obtain "two-dimensional" hydrodynamic force data for the models. This is accomplished by beginning the experimental tow with a small value of wetted length and increasing the wetted length in discrete steps, while measuring the hydrodynamic force at each step, all other experimental parameters held constant. As the wetted length is increased, the incremental increase in force per unit increase in wetted length eventually becomes constant (i.e., end effects become constant), and this constant ratio is the two-dimensional hydrodynamic force per unit length for the model at the particular speed and angle of inclination. In practice it is the force components, tangential and normal, which are of interest, and are measured. The data reduction procedure used to obtain the two-dimensional hydrodynamic force components is given below.

First, the force measurements, X and Z, are tabulated for each model in terms of the variables speed V, angle of inclination to the flow ϕ , and model wetted length s. An example of this tabulated data is given for Model G in Appendix A. As stated before, since these force measurements are generated by a three-dimensional model which pierces the water surface, the data contain both end effects and surface effects. To eliminate these effects the X and Z forces are plotted as a function of model wetted length for each angle and speed. As model wetted length increases, a length is reached beyond which both the X and Z forces become linear functions of wetted length for a given speed. Figure 16 typically shows, for a particular angle and discrete speeds, the change from a nonlinear to a linear relationship as s increases. Slopes of the linear portion of the force/wetted length curves are determined for each angle and speed. These slopes, $\Delta X/\Delta s$ and $\Delta Z/\Delta s$ represent the two-dimensional hydrodynamic forces per unit length acting on the faired cable model in the normal and tangential directions and are symbolized by F_n and F_t . Examples of these data, later used in deriving the hydrodynamic loading functions, are presented in tabular form in Appendix B.

In the cases of Models C, D, and I, the error associated with the small force measurement at very low speed (2 knots for Models C and D and 2 and 4 knots for Model I) precluded use of these data in formulating the loading functions.

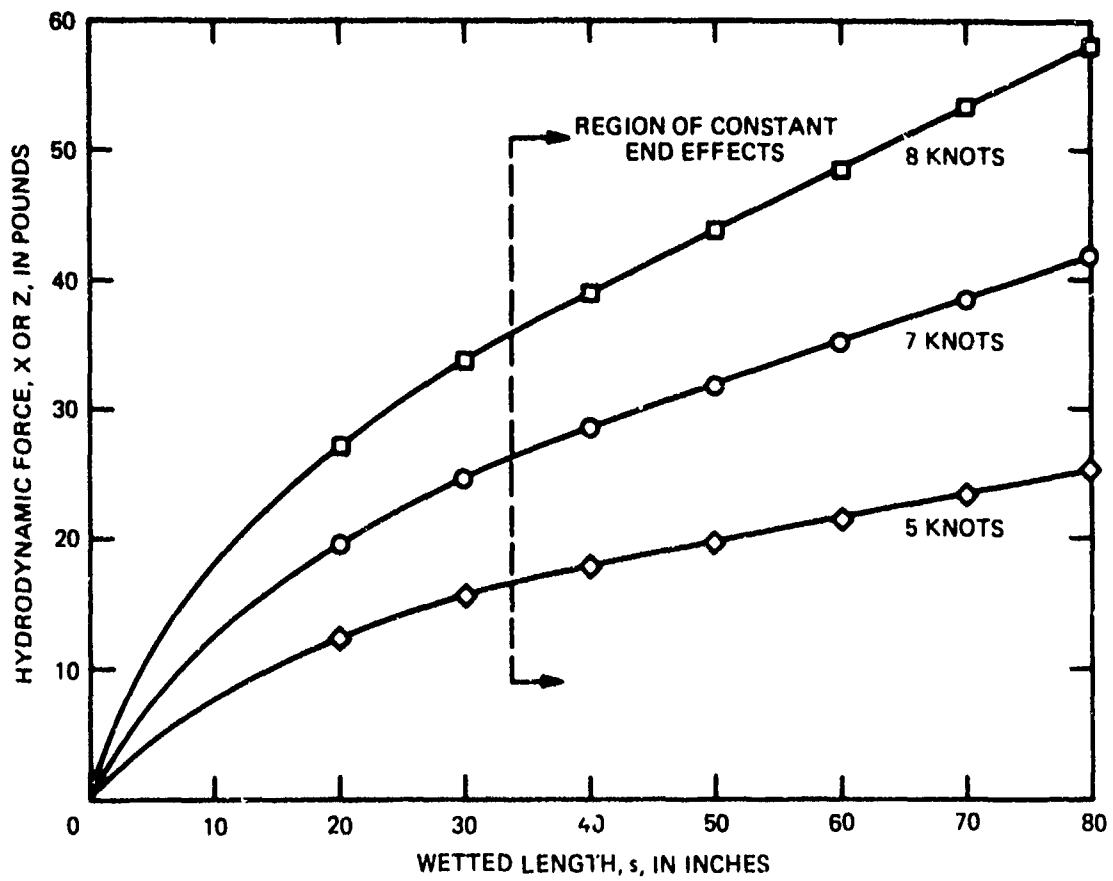


Figure 16 – Typical Curves of Hydrodynamic Force versus Wetted Length

HYDRODYNAMIC LOADING FUNCTIONS

As discussed above, the force measurements X and Z , were operated on to develop the two-dimensional hydrodynamic force components, F_n and F_t , per unit model length. However, the mathematical models used to compute the towline configuration generally accept the towline hydrodynamic loading terms in nondimensional form. It has therefore become customary to normalize the two-dimensional hydrodynamic force components per unit length by R , the normal force per unit length when $\phi = 90$ deg. When so normalized, these expressions

$$f_n = \frac{F_n}{R} \quad (1)$$

and

$$f_t = \frac{F_t}{R} \quad (2)$$

are referred to as the normal and tangential hydrodynamic loading functions, respectively. For a particular faired-cable geometry and speed, the loading functions are assumed to be dependent only on the angle ϕ . For the ten models the form of these expressions as functions of ϕ is such that they may be expressed analytically by selected combinations of the terms of the series,⁸

$$f(\phi) = A_0 + A_1 \cos \phi + B_1 \sin \phi + A_2 \cos 2\phi + B_2 \sin 2\phi \quad (3)$$

The details of processing of the data from tabulated force components to the final analytic series representation of the loading functions has not been treated uniformly for the ten fairing models. Essentially, two different methods have been used at the discretion of the particular analyst. The difference in method does not produce a substantive difference in results. In the first method (employed in all experiments except for Models C and D) the normal and tangential loading function values are obtained from the hydrodynamic force values. These values of F_n and F_t are divided by F_n at 90 degrees to obtain the normalized loading function values for each speed and angle. (Examples of these tabulated data are given in Appendix C.) A curve-fitting process is then performed on each set of normal and tangential

⁸Springston, G.B., "Generalized Hydrodynamic Loading Functions for Bare and Faired Cables in Two-Dimensional Steady-State Cable Configurations," NSRDC Report 2424 (Jun 1967).

values to obtain mathematical expressions for the loading functions. The curve-fitting process consists of generating a group of least-square fit curves for the loading function values with selected combinations of terms in the trigonometric series described by Equation (3) for which the boundary conditions are satisfied. The boundary conditions are given in Table 11. Finally, the curves in each group are compared with the data to determine the best form for each loading function.

In the second method, used for Models C and D, a least square curve fit is used to obtain the trigonometric series representation of the normal and tangential force data points at each speed. The boundary conditions specified are $f_n(0 \text{ deg}) = 0$, $df_n/d\phi(90 \text{ deg}) = 0$, and $f_t(90 \text{ deg}) = 0$. Data points are then extracted from these curves at 10 degree intervals over the range where measured data existed. These new data sets are normalized by dividing each value from the normal and tangential curves by the value of the normal curve at 90 deg for the same speed. A least squares curve fit again is made to the new data. The boundary conditions for this fit are as specified in Table 11.

DRAG COEFFICIENT

The drag coefficient, C_R , and corresponding Reynolds number, R_n are calculated for each speed by the following expressions:

$$C_R = \frac{R}{1/2 \rho t V^2} \quad (4)$$

and

$$R_n = \frac{V t}{\nu} \quad (5)$$

Note that in Equations (4) and (5) t is evaluated as the larger of the two dimensions, fairing thickness or cable diameter.

EXPERIMENTAL RESULTS

The previously described methods led to loading functions and drag coefficients for each model.

TABLE 11 – BOUNDARY CONDITIONS FOR ANALYTIC FUNCTIONS

Model	Boundary Conditions	
	Normal Loading Function	Tangential Loading Function
C, D, A, I	$f_n(0^0) = 0$ $\frac{df_n(90^0)}{d\phi} = 0$ $f_n(90^0) = 1$	$f_t(90^0) = 0$
B, G, E, F, H, J	$f_n(0^0) = 0$ $f_n(90^0) = 1$	$f_t(90^0) = 0$

The coefficients of the trigonometric series representing the normal and tangential loading functions for all the models are presented in Table 12. The functions are presented graphically in Appendix D.

Figure 17 presents smooth curve representations of C_R versus R_n for each model. Individual plots of C_R versus R_n showing data points for each model and the respective smooth curve from Figure 17 are included in Appendix E.

Model H was towed for all values of ϕ at only two speeds and was not towed at any additional speeds for the case of $\phi = 90$. The drag coefficient was calculated for the two speeds and compared to Model G which was identical except for the fairing clips. The drag coefficient was within four percent of the values of the curve determined for the drag coefficient for Model G. Since this is within the experimental scatter of Model G, the data for the curve of the drag coefficient of Model G was determined to be valid for Model H.

DISCUSSION

As stated in the Introduction, this measurement of the two-dimensional hydrodynamic loading functions by basin towing of short span fairing models is the first part of a program aimed at improving the capability of towline configuration prediction. The data presented herein document the work performed to date under this first part of the program. The ultimate worth of the data and the techniques which produced it remains to be proven by correlation with measurements on real faired towlines at sea. Therefore, no judgments as to the adequacy of the data and techniques can be made until the at-sea experiments have been conducted. Even in judging, on the basis of these data, the relative hydrodynamic efficiencies of the various shapes caution must be exercised. For example, radius of curvature may be an important parameter in the hydrodynamic loading on sectional fairing.

It should be mentioned that in representing the loading functions analytically the selection of the particular series terms used is somewhat arbitrary. Other analytical functions might better represent certain of the loading functions. Subsequent fairing model experimental results may require a different analytical representation. For the model experiments reported here, however, this representation is judged adequate and it promotes a uniformity convenient for computer use.

A second aspect of the analytical representation of the loading functions should be noted. The functions are defined over the interval of ϕ from 0 deg to 90 deg. Except for Model A, physical measurements were made only over the range of ϕ from 30 deg to 90 deg. Fairing is rarely used at shallow towing angles, however, so that the legitimacy of this extrapolation is not of practical importance.

TABLE 12 - HYDRODYNAMIC LOADING FUNCTION COEFFICIENTS

Model	Loading Function	Coefficients				
		$f(\phi) = A_0 + A_1 \cos\phi + B_1 \sin\phi + A_2 \cos 2\phi + B_2 \sin 2\phi$				
		A_0	A_1	B_1	A_2	B_2
A	f_n	0.2675	0	0.4650	-0.2675	0
	f_t	-2.3034	2.4536	2.4712	0.1678	-0.8232
B	f_n	-1.5716	1.7367	2.4065	-0.1651	-0.7808
	f_t	-0.1158	0.4641	0.1158	0	0
C	f_n	-1.0065	1.0670	1.9460	-0.0605	-0.5335
	f_t	-0.2165	0.6696	0	-0.2165	0
D	f_n	-3.5385	3.2217	4.8553	0.3168	-1.6109
	f_t	-0.1414	0.5394	0.1414	0	0
E	f_n	-0.5550	0.7733	1.3367	-0.2183	-0.4505
	f_t	-0.3544	0.4305	0.3862	0.0318	0
F	f_n	-1.0640	1.2633	1.8647	-0.1993	-0.6926
	f_t	0.2759	-0.1423	-0.2759	0	0.2120
G	f_n	1.2150	-1.1180	-0.3120	-0.0970	0.3070
	f_t	0.0172	0.4009	-0.0172	0	0
H	f_n	-1.4871	1.6969	2.2773	-0.2098	-0.8906
	f_t	-0.1615	0.2738	0.1615	0	0
I	f_n	-1.852	1.833	2.871	0.019	-0.917
	f_t	-2.157	2.797	2.019	-0.1379	-0.7623
J	f_n	1.1869	-1.1869	-0.1869	0	0.2751
	f_t	0.0223	0.2587	-0.0223	0	0

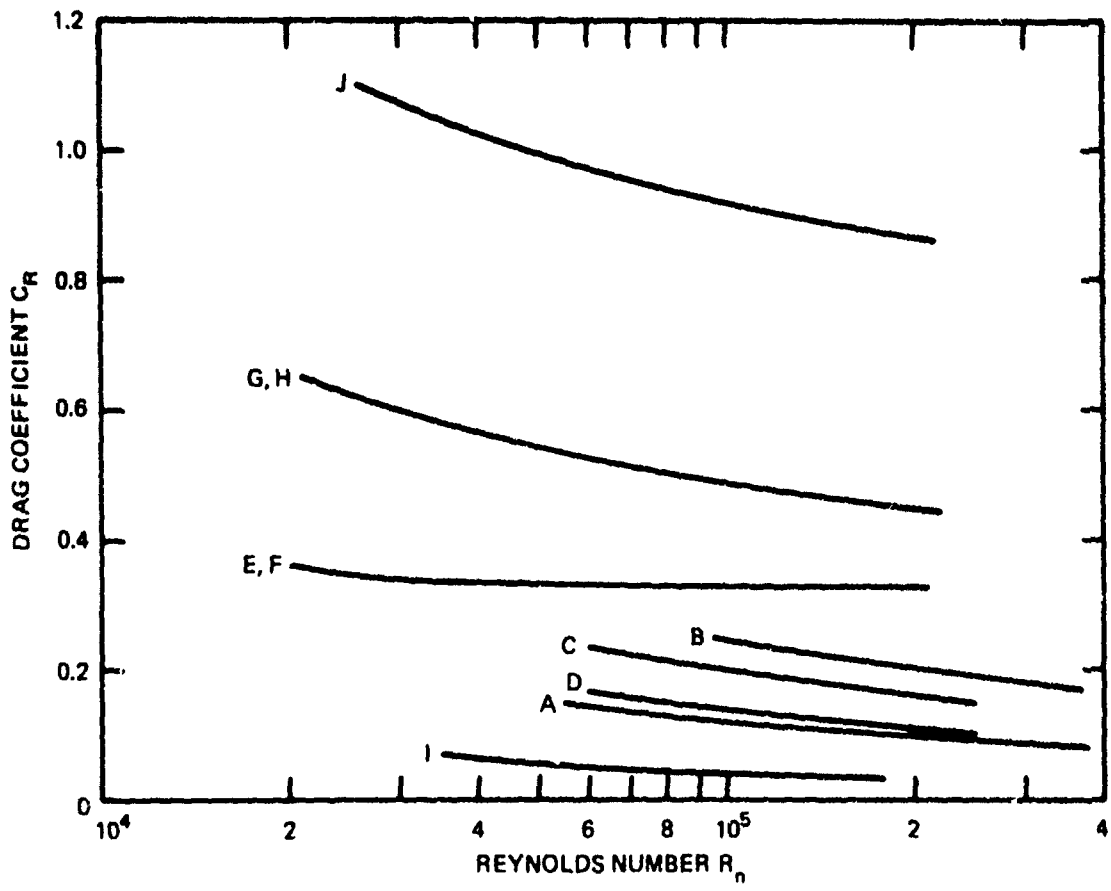


Figure 17 - Drag Coefficient versus Reynolds Number

CONCLUSIONS

Based on the results of these experiments, the following conclusion is drawn:

The DTMB Cable Fairing Dynamometer can be used with faired cable shapes to obtain loading functions and drag coefficients in such a form to permit comparison of the relative characteristics of the faired cable shapes.

It must be noted that the results contained in this report were obtained using large rigid models of various types of fairing for flexible cables. These results have not been validated for systems using the appropriate fairing. Such validation will be the subject of future reports.

ACKNOWLEDGMENTS

The work reported herein represents the individual efforts of the following members, past and present, of the Towed Systems Branch:

F.C. Belen
R.E. Brillhart
T. Gibbons
D.E. Gray
J.V. Mirabella
C.G. Walton

Much of this work has been done under the direction of the author, whose name has been used for cataloging purposes. In addition, the author wishes to recognize Mr. J.J. Nelligan of MAR, Associates for his assistance in compiling, organizing and writing this report.

APPENDIX A
TABLATED FORCE MEASUREMENT DATA

TABLE A.1 - EXPERIMENTAL DATA FOR THE FAIRED-CABLE MODEL G

Cable Angle, degrees	Speed, knots	Wetted Length, inches	Normal Force, pounds	Tangential Force, pounds
90.00*	0.80	85	1.22	
	0.80	85	1.28	
	0.79	76	1.08	
	0.81	76	1.16	
	0.80	65	0.94	
	0.79	65	0.92	
	0.81	53	0.80	
	0.79	53	0.76	
	0.81	42	0.64	
	0.79	42	0.60	
	1.01	85	2.20	
	1.10	85	2.20	
	1.01	76	1.80	
	1.05	76	2.00	
	1.01	65	1.64	
	1.02	65	1.66	
	0.99	53	1.30	
	1.02	53	1.36	
	0.98	42	0.96	
	1.05	42	1.06	
	1.52	85	3.44	
	1.52	85	3.44	
	1.52	76	3.08	
	1.55	76	3.34	
	1.50	76	2.94	
	1.50	65	2.58	
	1.49	65	2.56	
	1.50	53	2.16	
	1.50	53	2.16	
	1.50	42	1.90	
	1.48	42	1.80	
	2.01	85	6.40	
	2.04	85	6.60	
2.00	76	5.50		
2.00	76	5.70		
2.01	65	4.85		
2.01	65	4.84		
2.00	53	3.92		
2.01	53	3.96		
2.00	42	3.12		
2.05	42	3.37		

*The basin water temperature for these data was 70 degrees F. The temperature for all other data was 74 degrees F.

TABLE A.1 (Continued)

Cable Angle, degrees	Speed, knots	Wetted Length, inches	Normal Force, pounds	Tangential Force, pounds
90.00*	2.50	85	9.96	
	2.52	85	10.12	
	2.55	76	9.34	
	2.51	76	8.88	
	2.49	76	8.66	
	2.49	65	7.54	
	2.49	65	7.30	
	2.50	53	6.10	
	2.50	53	6.18	
	2.50	42	4.86	
	2.50	42	4.90	
	3.00	85	14.80	
	3.02	85	15.00	
	3.00	76	13.20	
	3.00	76	13.30	
	3.00	65	11.28	
	3.00	65	11.19	
	3.00	53	9.28	
	3.00	53	9.28	
	3.00	42	7.50	
	3.02	42	7.62	
	3.51	85	20.74	
	3.52	85	20.80	
	3.50	76	18.16	
	3.53	76	18.66	
	3.49	76	18.18	
	3.49	65	15.68	
	3.50	65	15.54	
	3.50	53	12.90	
	3.50	53	12.96	
	3.50	42	10.32	
	3.50	42	10.24	
	3.99	85	25.40	
	4.00	85	25.05	
	4.00	76	22.70	
	4.01	76	22.50	
	4.00	65	20.15	
	3.99	65	20.15	
	4.00	53	16.70	
	4.00	53	16.50	
	3.99	42	13.40	
	4.00	42	13.95	

*The basin water temperature for these data was 70 degrees F. The temperature for all other data was 74 degrees F.

TABLE A.1 (Continued)

Cable Angle, degrees	Speed, knots	Wetted Length, inches	Normal Force, pounds	Tangential Force, pounds
90.00*	4.51	85	32.55	
	4.53	85	32.50	
	4.51	76	29.00	
	4.53	76	29.00	
	4.51	65	24.80	
	4.50	65	24.65	
	4.52	53	21.25	
	4.49	53	20.95	
	4.51	42	17.25	
	4.51	42	16.95	
	5.02	85	41.20	
	5.02	85	41.90	
	5.01	75	36.80	
	5.05	76	36.70	
	5.01	65	31.40	
	5.02	65	31.40	
	5.01	53	26.10	
	5.02	53	26.05	
	5.02	42	21.55	
5.03	42	21.35		
90.00	5.01	76	36.00	3.00
	5.01	76	35.50	1.50
	5.01	65	31.00	1.50
	5.01	65	31.00	1.50
	5.01	53	25.00	2.00
	5.01	53	25.50	1.50
	5.01	42	20.50	2.00
	5.01	42	20.50	1.75
	5.01	30	16.00	2.00
	5.01	30	14.50	1.50
	5.01	30	16.00	1.25
	5.00	19	10.50	1.50
	5.01	19	10.50	1.50
	8.01	76	93.50	3.00
	8.01	76	93.00	3.00
	8.01	65	82.00	3.00
	8.01	65	82.00	3.00
	8.01	53	69.00	3.50
	8.01	53	69.00	3.00
	8.00	42	58.00	3.50
8.01	42	58.00	3.75	
*The basin water temperature for these data was 70 degrees F. The temperature for all other data was 74 degrees F.				

TABLE A.1 (Continued)

Cable Angle, degrees	Speed, knots	Wetted Length, inches	Normal Force, pounds	Tangential Force, pounds	
90.00	8.02	30	44.00	4.00	
	8.01	30	44.00	3.50	
	8.01	30	45.00	3.50	
	8.03	19	31.50	4.75	
	8.02	19	31.50	4.75	
79.73	5.01	76	34.00	4.10	
79.68	5.01	76	35.00	3.75	
	5.01	65	30.00	3.50	
	5.01	65	30.00	3.00	
	5.02	53	25.00	3.10	
	5.03	53	25.00	3.10	
	5.02	42	20.00	2.75	
	5.02	42	20.00	2.75	
	5.03	30	15.00	2.25	
	5.03	30	15.20	2.00	
	5.05	19	10.50	2.10	
	5.02	19	10.50	1.90	
79.73	8.00	76	90.00	8.00	
79.68	8.00	76	89.50	8.25	
	8.00	65	78.50	7.50	
	8.00	65	79.00	7.50	
	7.99	53	68.00	6.60	
	8.00	53	67.00	6.60	
	8.00	42	56.00	6.00	
	8.00	42	56.00	6.00	
	8.01	30	44.00	5.25	
	8.01	30	44.00	5.10	
	8.00	19	29.50	6.00	
	8.03	19	29.50	5.75	
	69.82	4.99	76	30.50	6.25
		4.98	76	30.50	6.00
5.00		65	26.40	5.60	
5.00		65	26.10	5.75	
5.00		53	22.00	4.50	
4.98		53	22.00	4.90	
5.00		42	18.00	4.10	
5.00		42	18.00	4.00	
5.01		30	13.80	3.25	
5.02		30	14.00	3.05	
5.00		19	9.10	2.50	
5.00		19	9.10	2.50	

TABLE A.1 (Continued)

Cable Angle, degrees	Speed, knots	Wetted Length, inches	Normal Force, pounds	Tangential Force, pounds
69.82	7.98	76	80.50	13.60
	7.99	76	80.50	13.55
	7.98	65	71.00	12.15
	8.00	65	71.00	12.00
	7.98	53	60.00	10.00
	8.00	53	60.90	10.25
	7.00	42	50.50	8.65
	8.00	42	50.50	8.60
	8.01	30	39.80	7.00
	7.99	30	40.00	7.00
	8.00	19	26.00	6.50
	8.00	19	26.00	6.50
64.87	5.01	76	27.50	7.75
	5.01	76	27.50	7.40
	5.01	65	23.60	6.60
	5.01	65	24.60	6.50
	5.01	53	19.70	5.70
	5.01	53	19.50	5.75
	5.01	42	16.00	4.60
	5.00	42	16.00	4.60
	5.00	30	12.20	3.75
	5.01	30	12.30	3.75
	5.01	19	8.60	3.05
	5.01	19	8.60	3.05
	8.00	76	74.20	17.00
	8.00	76	75.00	16.90
	8.00	65	65.00	14.75
	8.00	65	65.00	14.70
	8.00	53	55.50	12.40
	8.01	53	55.50	12.50
	8.01	42	46.50	10.00
	8.03	42	46.50	10.00
	8.00	30	36.50	8.20
	8.01	30	36.20	8.15
	8.01	19	24.00	7.15
8.03	19	24.00	7.05	
59.88	5.01	76	25.50	8.50
	5.00	76	25.00	8.50
	5.00	65	21.00	7.25
	5.00	65	21.00	7.25
	5.00	53	18.00	6.50
	5.01	53	18.00	5.75
	5.02	42	15.00	5.00
	5.02	42	14.50	5.50
	5.01	30	11.50	4.25
	5.01	30	11.20	4.50

TABLE A.1 (Continued)

Cable Angle, degrees	Speed, knots	Wetted Length, inches	Normal Force, pounds	Tangential Force, pounds
59.88	5.01	19	8.00	3.50
	5.01	19	8.00	3.50
	7.99	76	67.50	19.50
	8.00	76	67.50	19.50
	8.02	65	59.00	16.75
	8.02	65	59.00	16.75
	8.00	53	50.00	14.25
	8.00	53	50.50	13.50
	8.02	42	43.00	11.25
	8.00	42	42.50	11.75
	8.01	30	34.00	9.00
	8.01	30	33.50	9.25
	8.01	19	22.00	8.00
8.01	19	22.00	8.00	
54.92	5.02	76	23.50	9.00
	5.01	76	23.10	8.90
	5.01	65	20.00	8.10
	5.01	65	20.00	8.00
	5.01	53	16.80	6.75
	5.01	53	16.50	6.75
	5.01	42	13.60	5.80
	5.02	42	13.50	5.50
	5.02	30	10.20	4.25
	5.02	30	10.20	4.15
	5.00	19	6.80	3.00
	4.99	19	6.50	3.00
	8.02	76	63.50	20.75
	8.01	76	63.00	21.10
	8.01	65	54.80	18.50
	8.00	65	54.80	18.30
	8.00	53	46.50	15.40
	8.00	53	46.50	15.40
	8.01	42	39.20	12.25
	8.02	42	39.20	12.25
	8.01	30	30.80	9.25
8.00	30	30.50	9.25	
8.02	19	19.40	7.50	
8.01	19	19.20	7.50	
49.98	4.99	76	21.10	10.05
	5.00	76	21.60	10.25
	4.99	65	18.00	8.75
	5.02	65	18.50	9.00
	5.00	53	15.20	7.60
	5.00	53	15.00	7.50
	5.02	42	12.20	6.10

TABLE A.1 (Continued)

Cable Angle, degrees	Speed, knots	Wetted Length, inches	Normal Force, pounds	Tangential Force, pounds
49.98	5.01	42	12.20	6.10
	5.01	30	9.00	4.75
	5.01	30	9.00	4.50
	5.01	19	6.00	3.50
	5.01	19	6.00	3.50
	8.00	76	57.00	23.75
	7.99	76	57.00	24.00
	8.00	65	49.50	20.05
	7.99	65	49.50	20.00
	8.00	53	42.00	17.00
	8.00	53	41.60	17.00
	7.99	42	35.00	13.25
	8.00	42	35.00	13.20
	8.00	30	27.50	9.50
	8.00	30	27.50	9.75
8.00	19	17.00	7.75	
8.00	19	17.00	7.65	
40.10	5.00	76	16.10	11.50
	5.01	76	16.50	11.50
	5.01	65	14.00	10.25
	5.02	65	14.00	10.10
	5.02	53	11.25	8.50
	5.00	53	11.50	8.50
	5.01	42	9.25	6.60
	5.00	42	9.25	7.00
	5.01	30	6.90	5.40
	5.01	30	7.00	5.40
	5.00	19	4.50	3.50
	5.01	19	4.35	4.00
	8.00	76	43.00	26.50
	8.00	76	43.00	26.50
	8.00	65	37.25	23.60
	8.00	65	37.10	23.50
	8.01	53	30.50	19.50
	7.99	53	30.75	19.25
	8.00	42	26.00	14.60
	8.01	42	26.00	15.25
	8.00	30	20.38	11.10
	8.00	30	20.40	11.10
6.00	19	12.65	7.65	
8.00	19	12.50	7.85	

TABLE A.1 (Continued)

Cable Angle, degrees	Speed, knots	Wetted Length, inches	Normal Force pounds	Tangential Force, pounds
29.18	5.01	76	10.00	12.75
	5.01	76	10.00	12.50
	5.00	65	8.50	11.00
	5.01	65	8.50	11.00
	5.01	53	7.10	9.00
	5.01	53	7.00	9.00
	5.01	42	5.60	7.50
	5.01	42	5.75	7.25
	5.01	30	3.95	5.35
	5.00	30	4.10	5.35
	5.01	19	3.00	3.50
	4.99	19	2.75	3.50
	8.01	76	27.30	30.00
	8.01	76	27.50	29.80
	8.01	65	23.80	25.50
	8.01	65	23.80	25.50
	8.01	53	20.25	20.50
	8.01	53	20.20	20.50
	8.01	42	16.50	16.25
	8.01	42	16.50	16.10
	8.01	30	12.85	11.60
	7.99	30	12.85	11.50
8.00	19	7.50	7.00	
8.00	19	7.50	7.10	

APPENDIX B
TABULATED VALUES OF THE HYDRODYNAMIC FORCES

TABLE B.1 - TWO-DIMENSIONAL HYDRODYNAMIC FORCES ON MODEL A

Cable Angle, degrees	Speed, knots	Normal Force F_n , pounds per foot	Tangential Force F_t , pounds per foot
30.62	5	0.5266	0.5460
	8	1.0267	1.2368
40.58	5	0.6842	0.4868
	8	1.5344	1.0652
50.50	5	0.8641	0.4655
	8	1.8782	0.9044
60.12	5	1.1964	0.3630
	8	2.4649	0.7266
70.10	5	1.4026	0.2255
	8	No data, large lateral oscillations	
79.82	5	1.3077	0.2071
	8	2.8169	0.2715
	13	6.8185	0.4742
79.92	5	1.2942	0.1997
	8	2.8169	0.2715
	13	6.8185	0.4742
90.00	5	1.2915	0.0152
	8	2.8386	-0.0175
	13	6.6157	0.0108
0.00	5	-	0.3962
	8	-	0.9257
	13	-	2.2199

TABLE B.2 - TWO-DIMENSIONAL HYDRODYNAMIC FORCES ON MODEL B

Cable Angle, degrees	Normal Force F_n , pounds per foot			Tangential Force F_t , pounds per foot		
	Speed, knots			Speed, knots		
	2	4	6	2	4	6
30.58	0.321	0.850	1.787	0.250	0.678	1.872
40.38	0.406	1.110	2.301	0.217	0.580	1.653
50.47	0.526	1.395	2.856	0.184	0.500	1.501
59.90	0.622	1.633	3.392	0.160	0.435	1.261
69.83	0.748	1.931	4.050	0.102	0.260	0.609
79.73	0.784	2.059	4.241	0.045	0.181	0.544
89.88	0.807	2.107	4.356	0	0	0

TABLE B.3 – TWO-DIMENSIONAL HYDRODYNAMIC FORCES ON MODEL C

Cable Angle, degrees	Normal Force F_n , pounds per foot				Tangential Force F_t , pounds per foot		
	Speed, knots				Speed, knots		
	2	4	6	8	4	6	8
89.7	0.604	2.00	3.79	6.20	-----	-----	-----
84.9	-----	1.85	3.69	6.03	0.145	0.289	0.566
79.8	-----	1.99	3.68	6.17	0.182	0.428	0.766
74.9	-----	1.75	3.91	-----	0.256	0.676	1.02
70.0	-----	1.81	3.92	5.74	0.191	0.682	0.954
60.2	-----	1.55	3.77	5.33	0.384	0.863	1.56
50.4	-----	1.19	2.69	3.82	0.460	1.10	1.63
40.5	-----	1.12	1.81	2.75	0.365	1.06	1.85
30.6	-----	0.916	1.75	1.96	0.391	1.21	-----

TABLE B.4 – TWO-DIMENSIONAL HYDRODYNAMIC FORCES ON MODEL D

Cable Angle, degrees	Normal Force F_n , pounds per foot				Tangential Force F_t , pounds per foot		
	Speed, knots				Speed, knots		
	2	4	6	8	4	6	8
89.7	0.411	1.34	3.30	4.11	-----	-----	-----
69.7	-----	1.23	2.18	3.03	0.198	0.554	0.736
50.7	-----	0.941	1.75	2.69	0.334	0.893	1.70
40.3	-----	0.763	1.39	2.23	0.385	0.911	1.73
30.3	-----	-----	-----	1.44	0.397	1.16	2.13

TABLE B.5 - TWO-DIMENSIONAL HYDRODYNAMIC FORCES ON MODEL E

Cable Angle, degrees	Normal Force F_n , pounds per foot							
	Speed, knots							
	2.5	3.0	3.5	4.0	5.0	5.5	6.0	6.5
30.40	0.296	0.430	0.572	0.694	1.037	1.321	1.495	1.712
35.30	0.361	0.438	0.654	0.783	1.225	1.552	1.816	2.133
40.30	0.401	0.604	0.755	0.996	1.539	1.826	2.198	2.609
45.20	0.437	0.692	0.872	1.164	1.788	2.180	2.644	3.021
50.10	0.551	0.790	1.046	1.342	2.071	2.580	2.996	3.524
55.10	0.598	0.867	1.107	1.485	2.286	2.855	3.321	3.969
60.10	0.702	1.001	1.342	1.700	2.690	3.296	3.808	4.495
64.85	0.759	1.083	1.448	1.875	2.971	3.636	4.300	4.985
69.85	0.825	1.148	1.557	1.966	3.089	3.882	4.421	5.247
74.80	0.859	1.222	1.673	2.121	3.343	4.134	4.799	5.604
79.70	0.901	1.270	1.754	2.198	3.446	4.311	4.994	5.984
84.70	0.936	1.333	1.831	2.346	3.621	4.392	5.219	6.143

Cable Angle, degrees	Tangential Force F_t , pounds per foot							
	Speed, knots							
	2.5	3.0	3.5	4.0	5.0	5.5	6.0	6.5
30.40	0.211	0.252	0.413	0.532	0.835	1.006	1.192	1.397
35.30	0.223	0.321	0.440	0.560	0.892	1.088	1.281	1.509
40.30	0.227	0.317	0.422	0.541	0.845	1.006	1.193	1.404
45.20	0.227	0.317	0.421	0.549	0.849	1.012	1.204	1.415
50.10	0.206	0.281	0.389	0.499	0.763	0.923	1.091	1.271
55.10	0.192	0.281	0.383	0.494	0.708	0.943	1.121	1.317
60.10	0.162	0.233	0.313	0.419	0.648	0.771	0.925	1.086
64.85	0.146	0.207	0.289	0.362	0.561	0.685	0.815	0.952
69.85	0.133	0.192	0.263	0.345	0.535	0.644	0.768	0.897
74.80	0.098	0.131	0.172	0.229	0.346	0.416	0.495	0.576
79.70	0.087	0.113	0.153	0.199	0.298	0.351	0.424	0.494
84.70	0.051	0.073	0.092	0.121	0.187	0.216	0.251	0.304

TABLE B.5 (Continued)

Cable Angle, degrees	Speed, knots	Normal Force F_n , pounds per foot	Tangential Force F_t , pounds per foot
89.94	1.0	0.196	0
	1.5	0.345	0
	2.0	0.589	0
	2.5	0.940	0
	3.0	1.347	0
	3.5	1.842	0
	4.0	2.400	0
	4.5	3.018	0
	5.0	3.733	0
	5.5	4.476	0
	6.0	5.363	0
	6.5	6.235	0
	7.0	7.191	0

TABLE B.6 – TWO-DIMENSIONAL HYDRODYNAMIC FORCES ON MODEL I

Cable Angle, degrees	Normal Force F_n , pounds per foot				
	Speed, knots				
	2	4	6	8	10
29.87	0.040	0.310	0.470	0.700	1.000
34.83	0.080	0.380	0.560	0.685	0.980
39.87	0.085	0.333	0.580	0.750	1.000
44.83	0.101	0.400	0.600	0.860	1.100
49.75	0.125	0.370	0.675	1.060	1.450
59.90	0.152	0.420	0.760	1.260	1.850
69.81	0.166	0.475	0.875	1.420	2.04
74.90	0.165	0.500	0.930	1.500	2.17
79.79	0.180	0.525	0.963	1.650	2.20
84.81	0.183	0.533	0.988	1.730	2.25
Cable Angle, degrees	Tangential Force F_t , pounds per foot				
	Speed, knots				
	2	4	6	8	10
29.87	0.063	0.170	0.550	0.910	1.300
34.83	0.100	0.185	0.533	0.933	1.300
39.87	0.085	0.233	0.530	0.875	1.100
44.83	0.062	0.195	0.450	0.940	0.950
49.75	0.071	0.240	0.480	0.810	1.120
59.90	0.028	0.205	0.410	0.715	0.940
69.81	-----	0.142	0.316	0.590	0.780
74.90	0.031	0.125	0.258	0.433	0.520
79.79	-----	-----	0.191	-----	0.365
84.81	0.014	0.046	0.116	0.166	0.185

TABLE B.6 (Continued)

Cable Angle, degrees	Speed, knots	Normal Force F_n , pounds per foot ⁿ	Tangential Force F_t , pounds per foot
89.94	2	0.185	0
	3	0.333	0
	4	0.536	0
	5	0.785	0
	6	1.000	0
	7	1.300	0
	8	1.750	0
	10	2.26	0

APPENDIX C
TABULATED VALUES OF THE LOADING FUNCTIONS

**TABLE C.1 – VALUES OF NORMALIZED NORMAL AND TANGENTIAL
LOADING FUNCTION FOR MODEL B**

Cable Angle, degrees	Normal f_n			Tangential f_t		
	Speed, knots			Speed, knots		
	2	4	6	2	4	6
30.58	0.400	0.405	0.409	0.313	0.323	0.420
40.38	0.500	0.525	0.520	0.271	0.276	0.380
50.47	0.650	0.657	0.655	0.200	0.207	0.290
59.90	0.775	0.776	0.779	0.200	0.207	0.290
69.83	0.925	0.920	0.925	0.125	0.128	0.140
79.73	0.975	0.976	0.975	0.056	0.086	0.125
89.88	1.000	1.000	1.000	0	0	0

TABLE C.2 - VALUES OF NORMALIZED NORMAL AND TANGENTIAL LOADING FUNCTION FOR MODEL E

Cable Angle, degrees	Normal f_n							
	Speed, knots							
	2.5	3.0	3.5	4.0	5.0	5.5	6.0	6.5
30.40	0.315	0.319	0.311	0.289	0.278	0.295	0.279	0.274
35.30	0.384	0.375	0.355	0.326	0.328	0.347	0.339	0.342
40.30	0.426	0.448	0.410	0.415	0.412	0.408	0.410	0.418
45.20	0.465	0.514	0.473	0.485	0.479	0.487	0.493	0.484
50.10	0.586	0.586	0.568	0.559	0.555	0.576	0.559	0.565
55.10	0.636	0.644	0.601	0.619	0.612	0.638	0.619	0.636
60.10	0.747	0.743	0.729	0.708	0.721	0.736	0.710	0.721
64.85	0.807	0.804	0.786	0.781	0.796	0.812	0.802	0.800
69.85	0.878	0.852	0.845	0.819	0.827	0.867	0.824	0.841
74.80	0.914	0.907	0.908	0.884	0.895	0.923	0.895	0.899
79.70	0.958	0.943	0.952	0.915	0.923	0.963	0.931	0.960
84.70	0.996	0.990	0.994	0.978	0.970	0.981	0.973	0.985
89.94	1.000	1.000	1.000	1.000	1.000	1.000	1.000	1.000
Cable Angle, degrees	Tangential f_t							
	Speed, knots							
	2.5	3.0	3.5	4.0	5.0	5.5	6.0	6.5
30.40	0.225	0.222	0.225	0.223	0.221	0.223	0.222	0.222
35.30	0.234	0.237	0.238	0.233	0.238	0.241	0.238	0.240
40.30	0.234	0.230	0.228	0.225	0.225	0.223	0.222	0.224
45.20	0.234	0.230	0.228	0.225	0.225	0.225	0.223	0.226
50.10	0.212	0.207	0.206	0.204	0.203	0.205	0.203	0.203
55.10	0.202	0.207	0.206	0.204	0.187	0.210	0.208	0.210
60.10	0.170	0.170	0.158	0.170	0.171	0.172	0.171	0.173
64.85	0.148	0.148	0.152	0.150	0.150	0.151	0.151	0.152
69.85	0.138	0.141	0.141	0.141	0.141	0.142	0.141	0.142
74.80	0.096	0.096	0.097	0.091	0.091	0.091	0.091	0.091
79.70	0.085	0.081	0.081	0.079	0.077	0.078	0.078	0.078
84.70	0.053	0.051	0.048	0.050	0.048	0.046	0.046	0.048
89.94	0.000	0.000	0.000	0.000	0.000	0.000	0.000	0.000

TABLE C.3 – VALUES OF NORMALIZED NORMAL AND TANGENTIAL LOADING FUNCTION FOR MODEL F

Cable Angle, degrees	Normal f_n				Tangential f_t			
	Speed, knots				Speed, knots			
	2	4	6	8	2	4	6	8
30.17	0.265	0.267	0.263	0.261	0.218	0.203	0.191	0.181
35.30	0.312	0.327	0.326	0.326	0.223	0.205	0.192	0.180
40.25	0.390	0.395	0.396	0.393	0.223	0.205	0.191	0.177
45.10	0.450	0.464	0.463	0.465	0.218	0.201	0.188	0.166
50.03	0.533	0.532	0.527	0.527	0.208	0.194	0.172	0.151
54.97	0.591	0.597	0.600	0.600	0.197	0.182	0.153	0.143
59.95	0.669	0.682	0.682	0.685	0.180	0.167	0.131	0.112
64.98	0.759	0.762	0.761	0.758	0.159	0.146	0.111	0.095
69.88	0.830	0.837	0.833	0.832	0.133	0.122	0.089	0.073
74.92	0.878	0.889	0.886	0.887	0.105	0.096	0.064	0.054
79.85	0.946	0.949	0.941	0.943	0.075	0.068	0.033	0.030
84.90	0.958	0.976	0.976	0.974	0.043	0.039	0.022	0.009
90.00	1.000	1.000	1.000	1.000	0	0	0	0

TABLE C.4 – VALUES OF NORMALIZED NORMAL AND TANGENTIAL LOADING FUNCTION FOR MODEL H

Cable Angle, degrees	Normal f_n		Tangential f_t	
	Speed, knots		Speed, knots	
	4	5	4	5
30.27	0.242	0.228	0.167	0.153
40.22	0.404	0.361	0.168	0.144
50.07	0.541	0.499	0.127	0.120
60.13	0.675	0.615	0.115	0.103
70.02	0.843	0.797	0.102	0.093
79.90	0.988	0.928	0.064	0.043
90.00	1.000	1.000	0	0

TABLE C.5 – VALUES OF NORMALIZED NORMAL AND TANGENTIAL LOADING FUNCTION FOR MODEL I

Cable Angle, degrees	Normal f_n				
	Speed, knots				
	2	4	6	8	10
29.87	0.216	0.590	0.470	0.400	0.440
34.83	0.432	0.708	0.560	0.391	0.433
39.87	0.459	0.621	0.580	0.428	0.442
44.83	0.545	0.746	0.590	0.491	0.491
49.75	0.675	0.690	0.625	0.620	0.641
59.90	0.821	0.783	0.760	0.720	0.820
69.81	0.864	0.886	0.875	0.811	0.902
74.90	0.987	0.932	0.930	0.857	0.960
79.79	0.972	0.979	0.963	0.942	0.973
84.81	0.983	0.994	0.988	0.988	0.995
89.94	1.000	1.000	1.000	1.000	1.000
Cable Angle, degrees	Tangential f_t				
	Speed, knots				
	2	4	6	8	10
29.87	0.340	0.315	0.550	0.520	0.575
34.83	0.540	0.345	0.533	0.533	0.560
39.87	0.460	0.435	0.530	0.500	0.486
44.83	0.360	0.363	0.450	0.530	0.393
49.75	0.394	0.447	0.480	0.450	0.490
59.90	0.170	0.385	0.410	0.395	0.415
69.81	-----	0.280	0.316	0.338	0.345
74.90	0.172	0.233	0.258	0.240	0.229
79.79	-----	-----	0.191	-----	0.162
84.81	0.078	0.090	0.105	0.093	0.081
89.94	0.000	0.000	0.000	0.000	0.000

TABLE C.6 - VALUES OF NORMALIZED NORMAL AND TANGENTIAL
LOADING FUNCTION FOR MODEL J

Cable Angle, degrees	Normal f_n				Tangential f_t			
	Speed, knots				Speed, knots			
	5	6	7	8	5	6	7	8
30.26	0.237	0.258	0.241	0.271	0.256	0.220	0.237	0.235
40.23	0.433	0.416	0.370	0.369	0.226	0.195	0.183	0.188
50.04	0.585	0.585	0.571	0.635	0.195	0.154	0.167	0.198
60.14	0.689	0.685	0.672	0.721	0.110	0.127	0.135	0.124
69.94	0.842	0.796	0.805	0.905	0.095	0.096	0.113	0.116
79.87	0.862	0.846	0.873	0.827	0.030	0.040	0.036	0.020
90.00	1.000	1.000	1.000	1.000	0	0	0	0

APPENDIX D
GRAPHS OF THE HYDRODYNAMIC LOADING FUNCTIONS

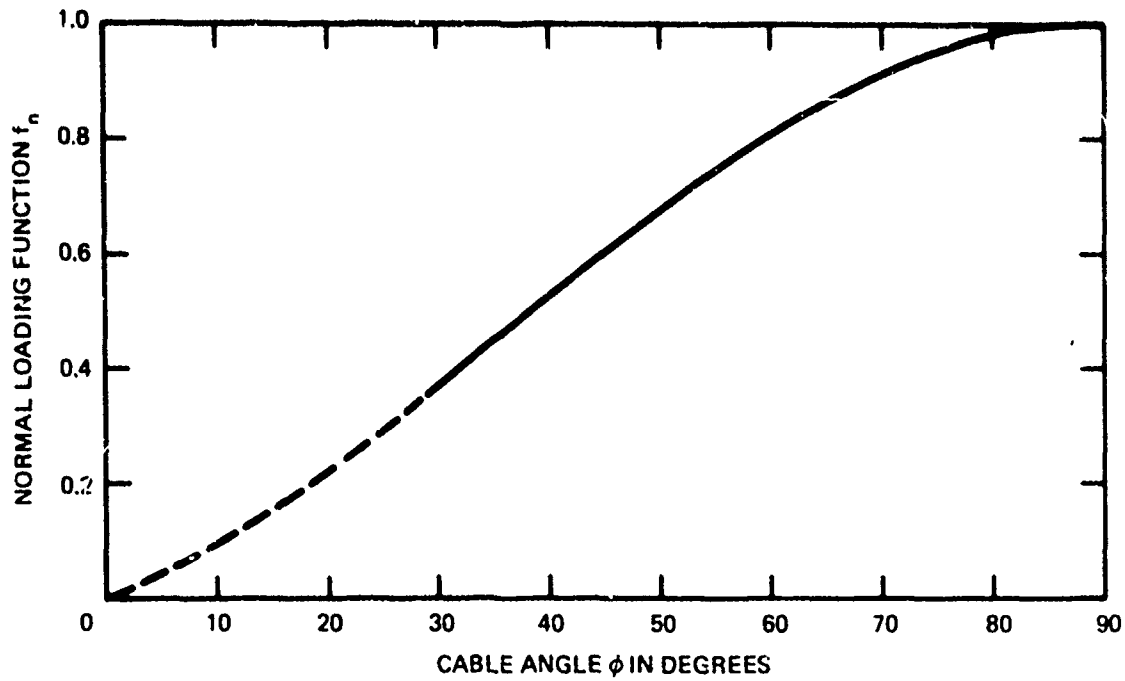


Figure D.1 – Normal Loading Function f_n versus Cable Angle for Model A

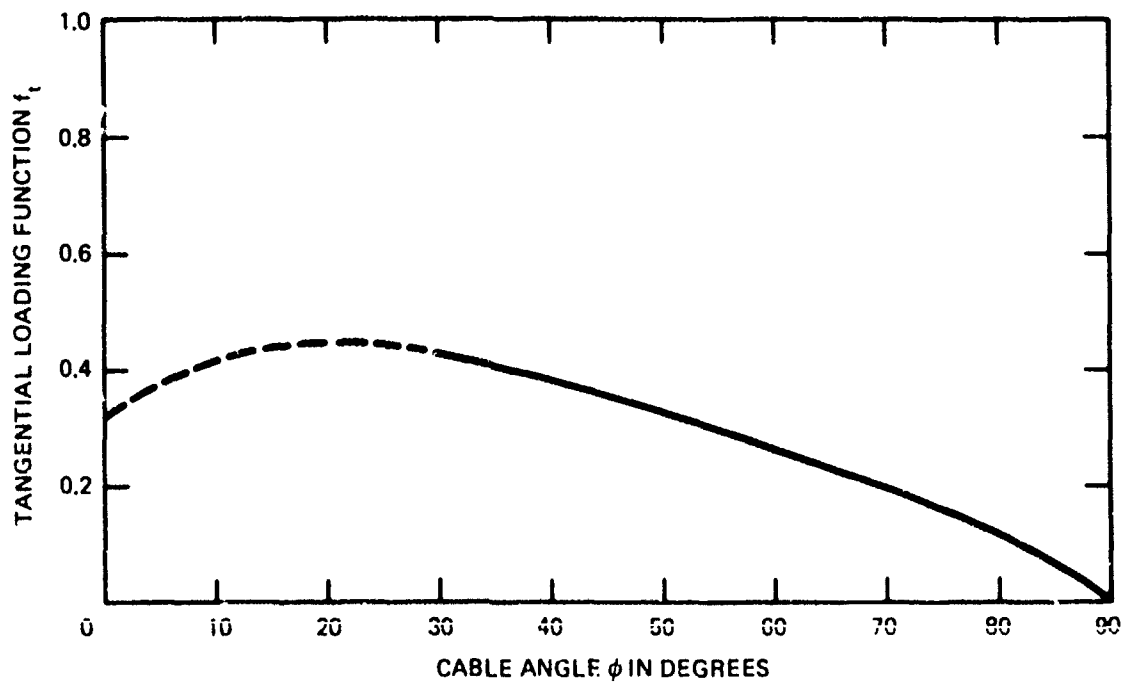


Figure D.2 – Tangential Loading Function f_t versus Cable Angle for Model A

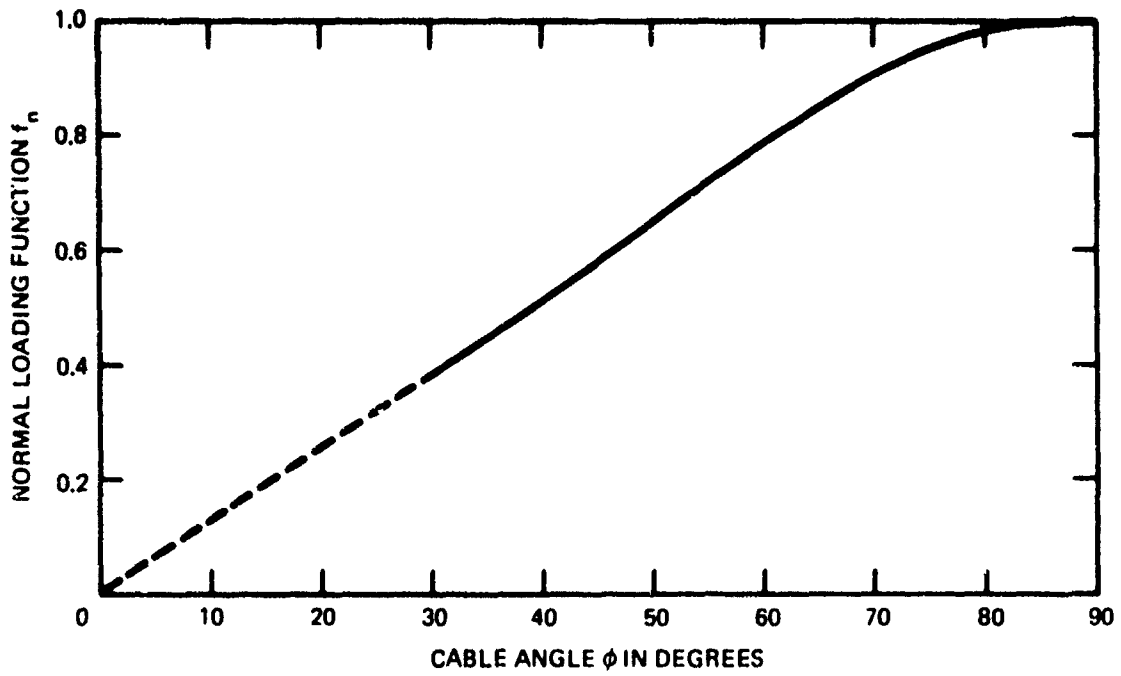


Figure D.3 - Normal Loading Function f_n versus Cable Angle for Model B

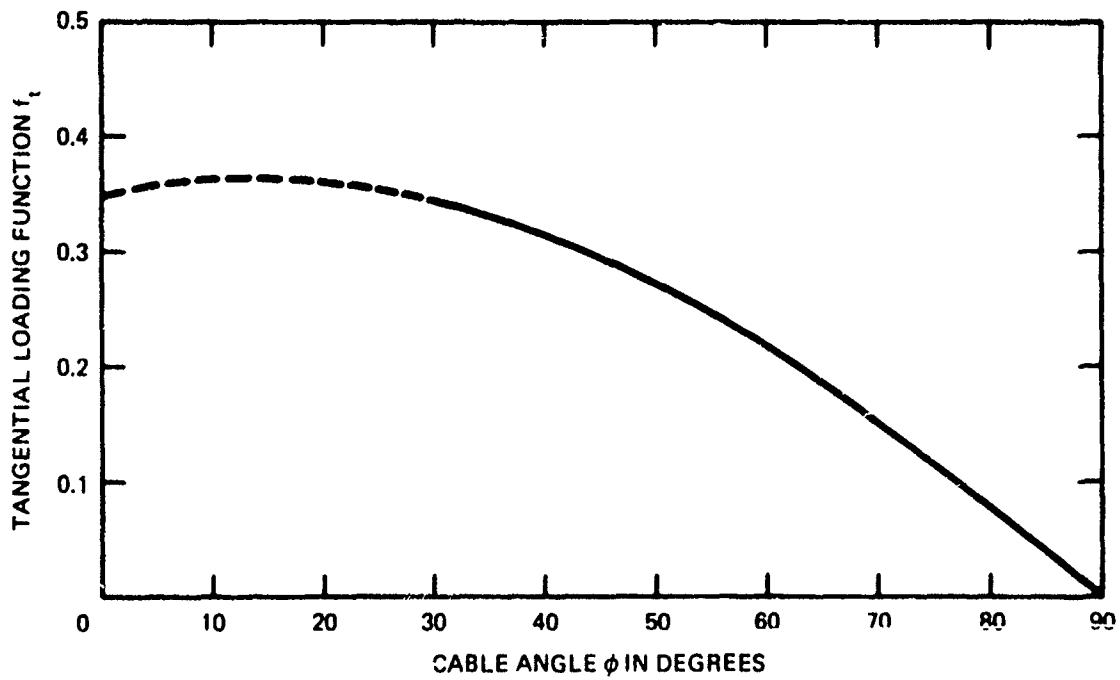


Figure D.4 - Tangential Loading Function f_t versus Cable Angle for Model B

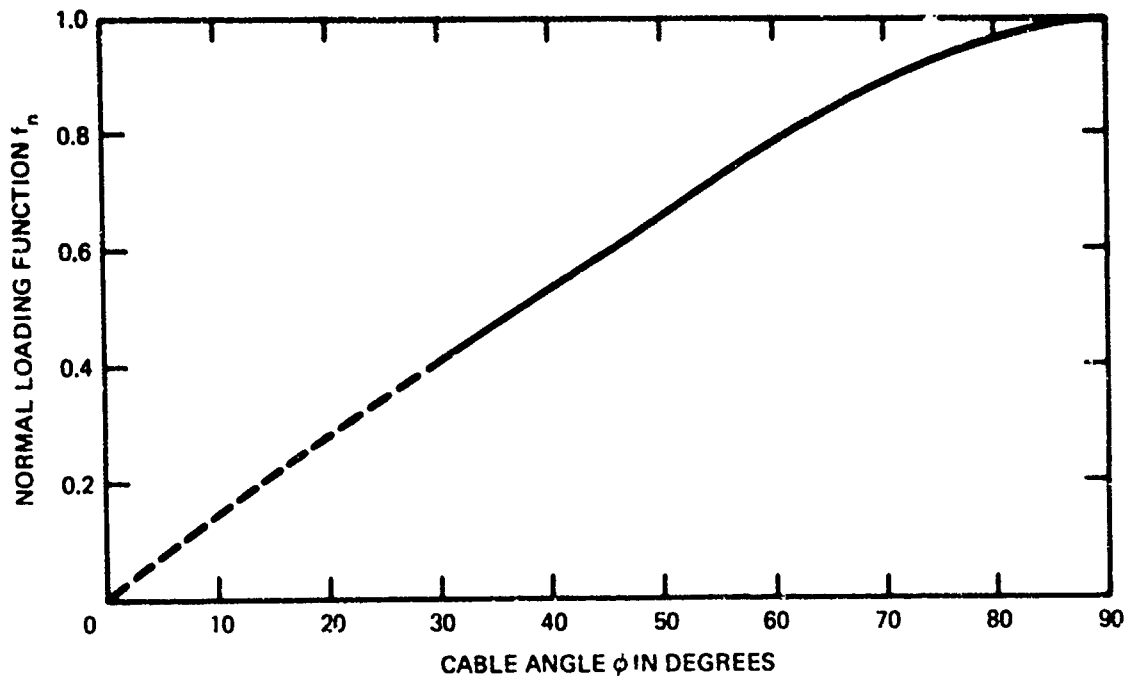


Figure D.5 – Normal Loading Function f_n versus Cable Angle for Model C

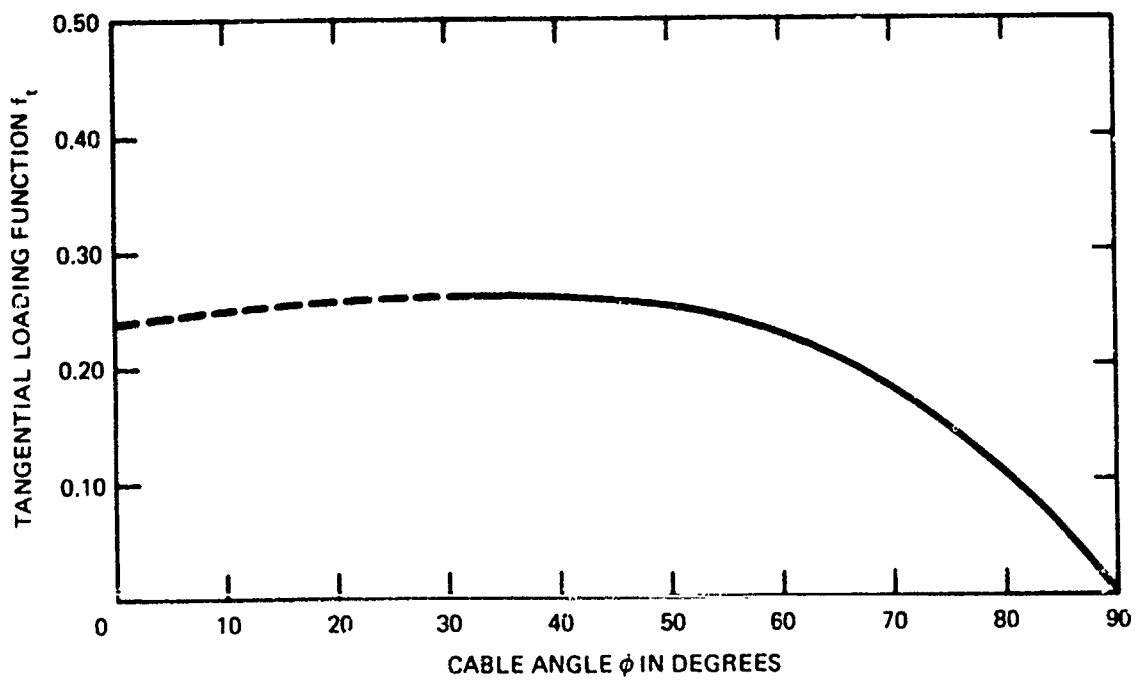


Figure D.6 – Tangential Loading Function f_t versus Cable Angle for Model C

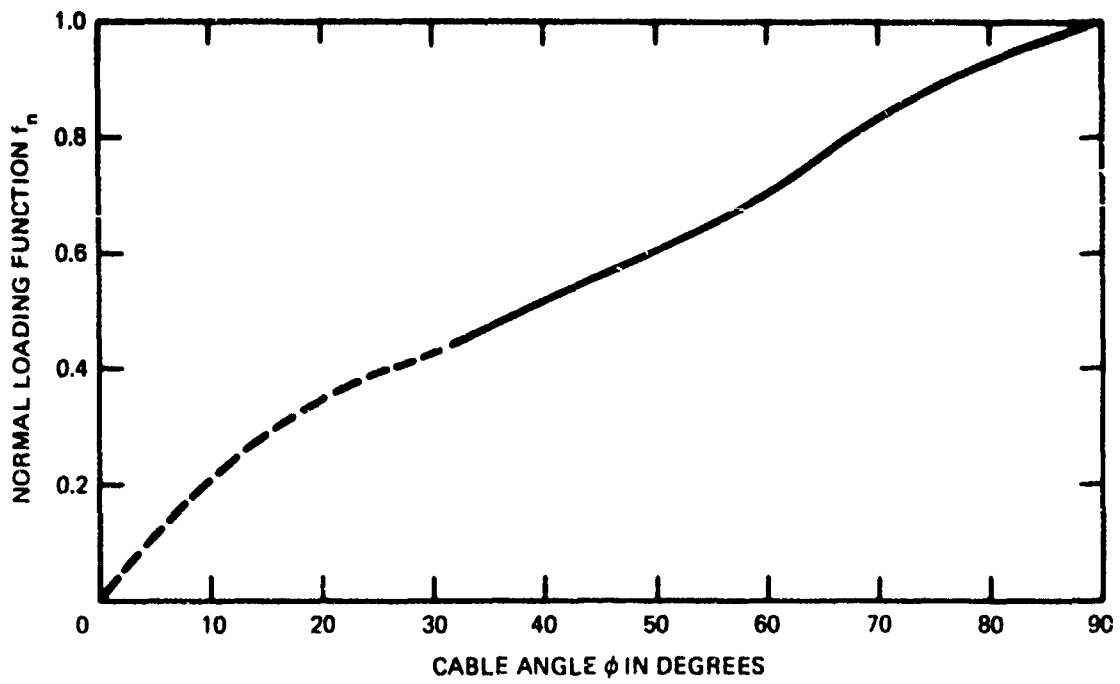


Figure D.7 – Normal Loading Function f_n versus Cable Angle for Model D

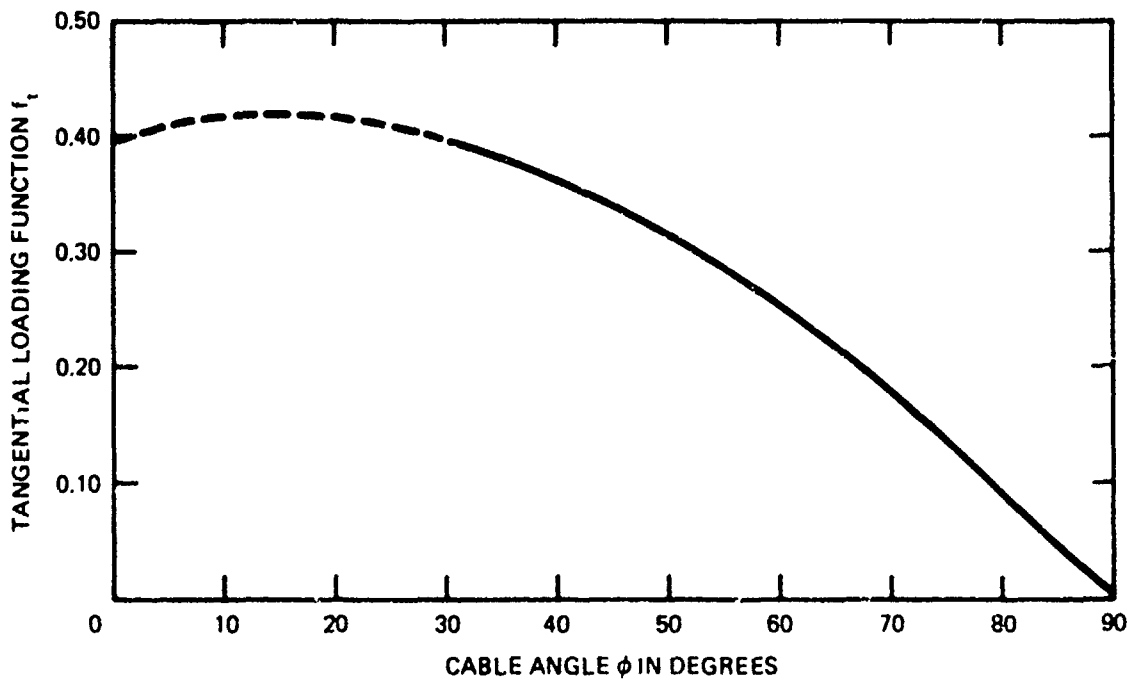


Figure D.8 – Tangential Loading Function f_t versus Cable Angle for Model D

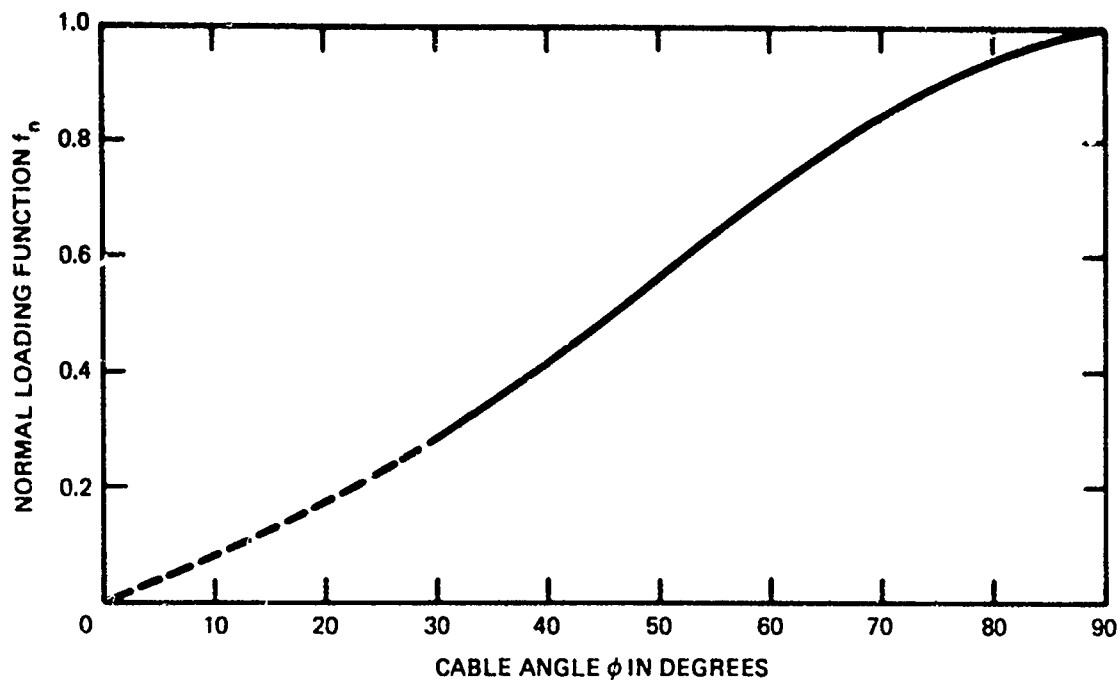


Figure D.9 – Normal Loading Function f_n versus Cable Angle for Model E

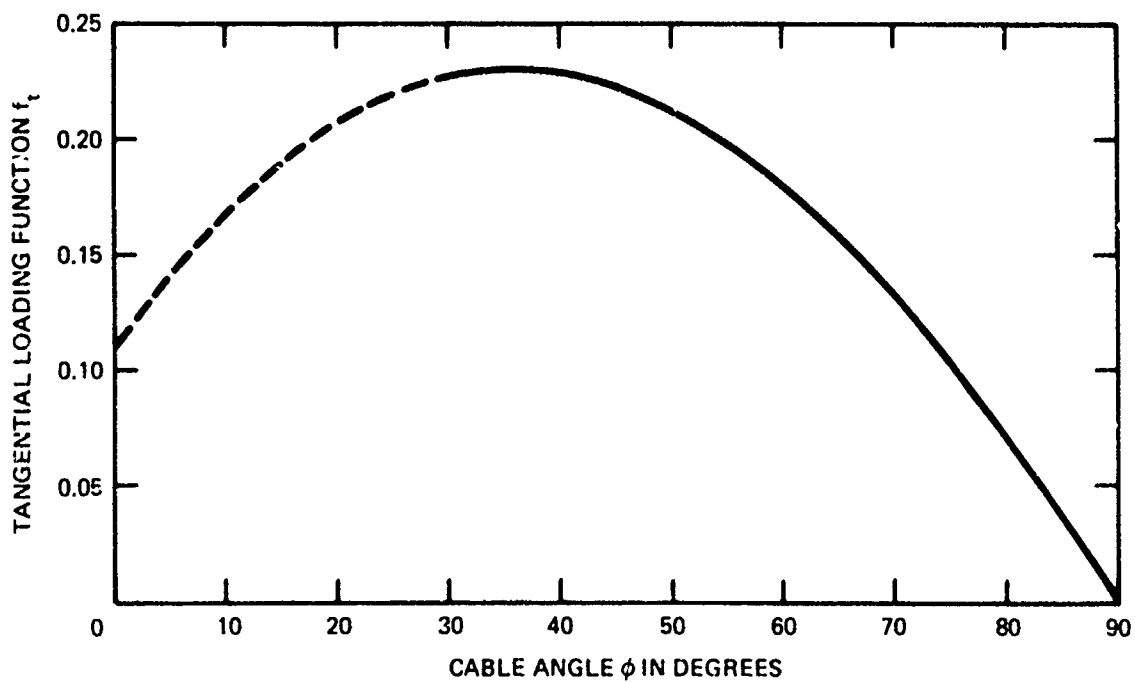


Figure D.10 – Tangential Loading Function f_t versus Cable Angle for Model E

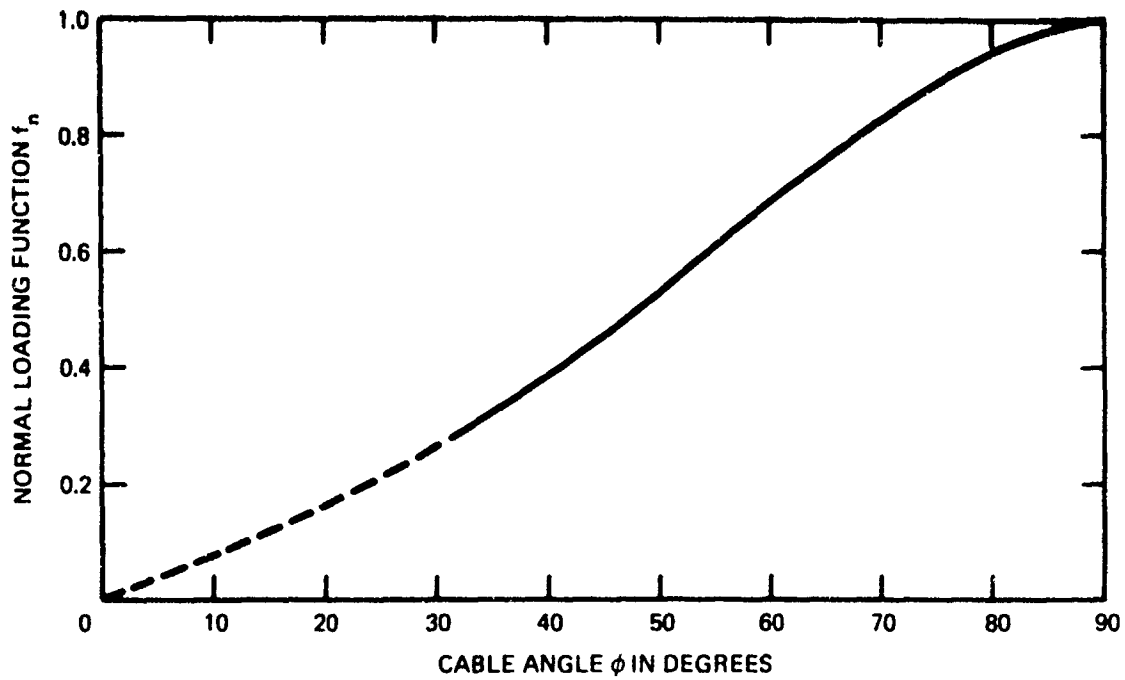


Figure D.11 – Normal Loading Function f_n versus Cable Angle for Model F

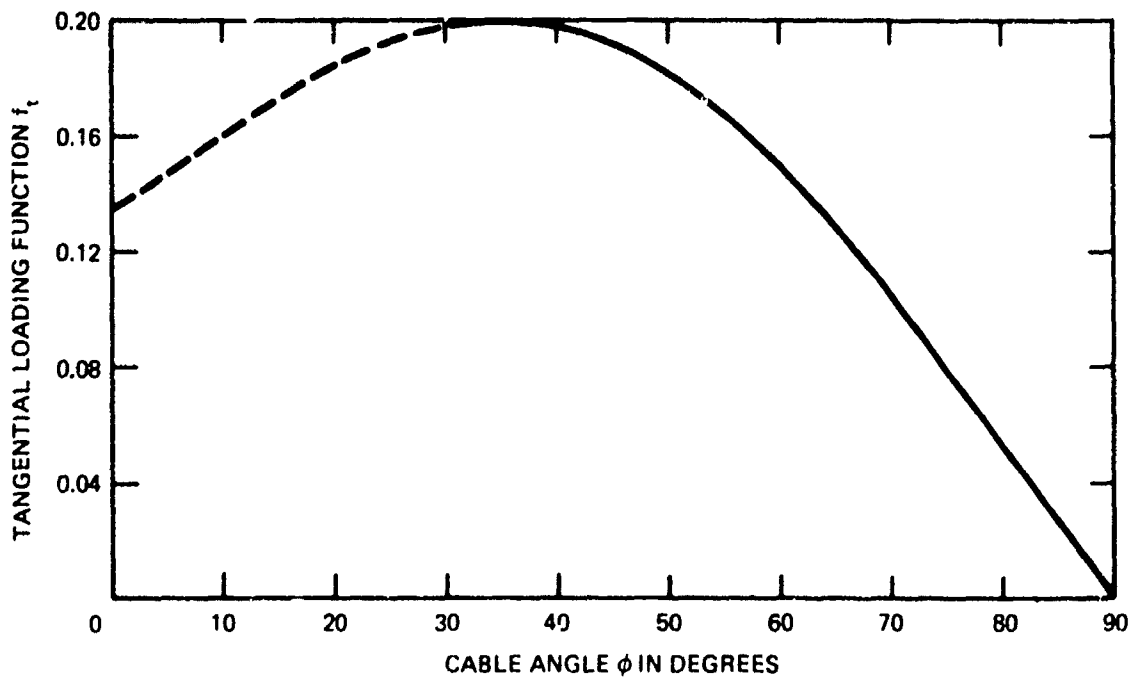


Figure D.12 – Tangential Loading Function f_t versus Cable Angle for Model F

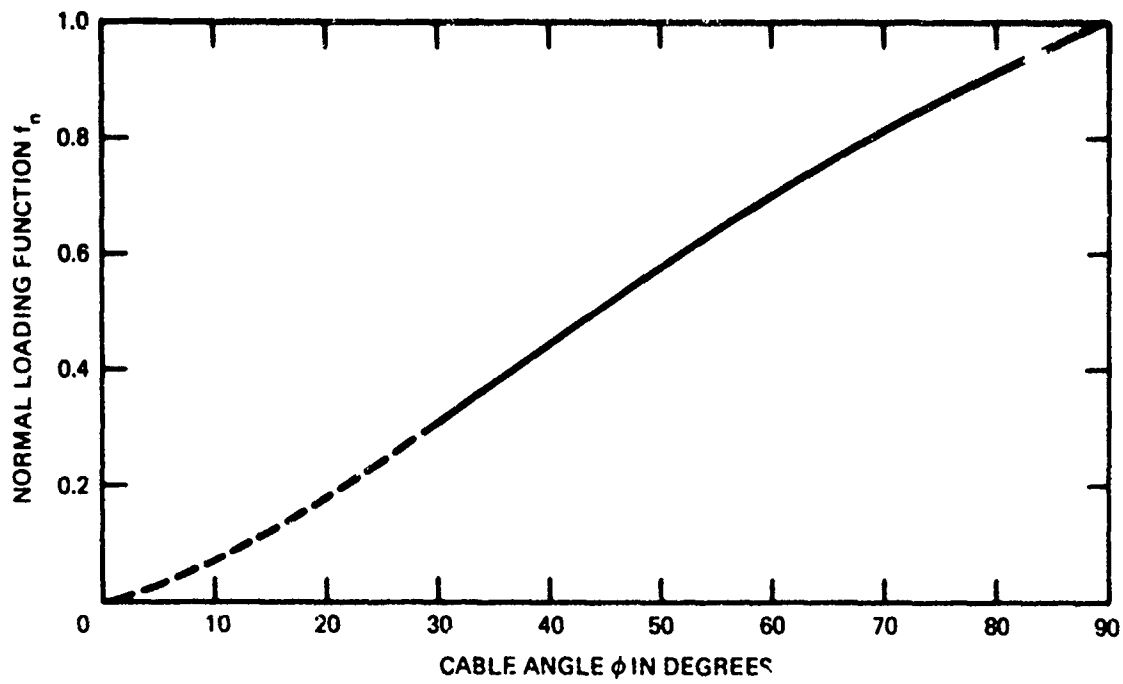


Figure D.13 – Normal Loading Function f_n versus Cable Angle for Model G

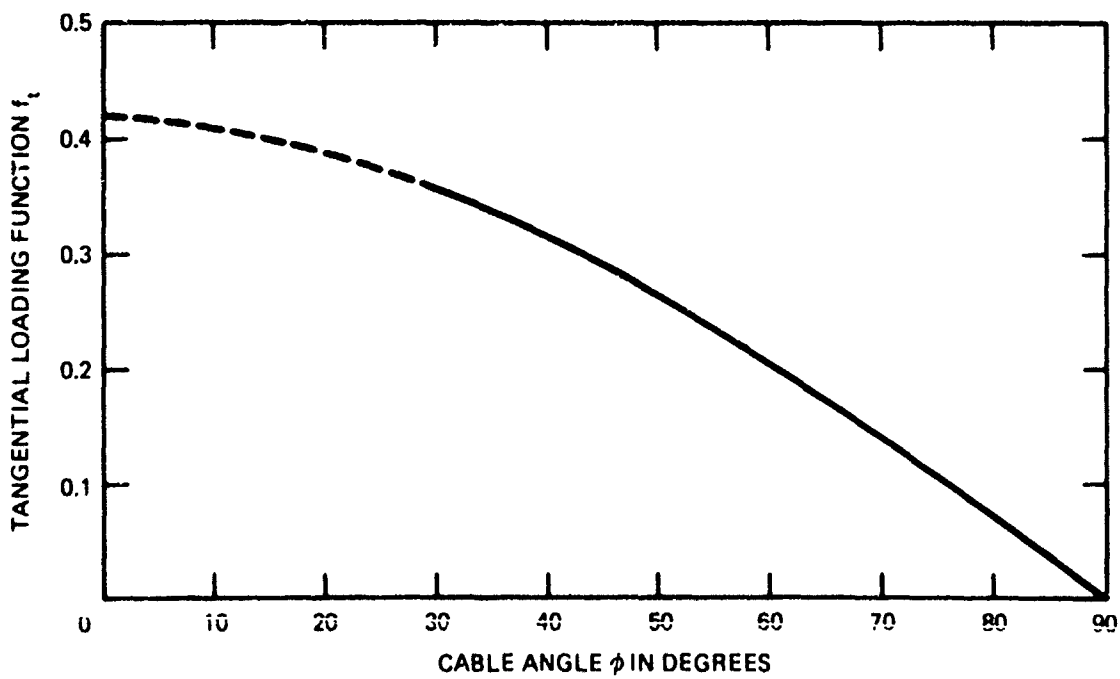


Figure D.14 – Tangential Loading Function f_t versus Cable Angle for Model G

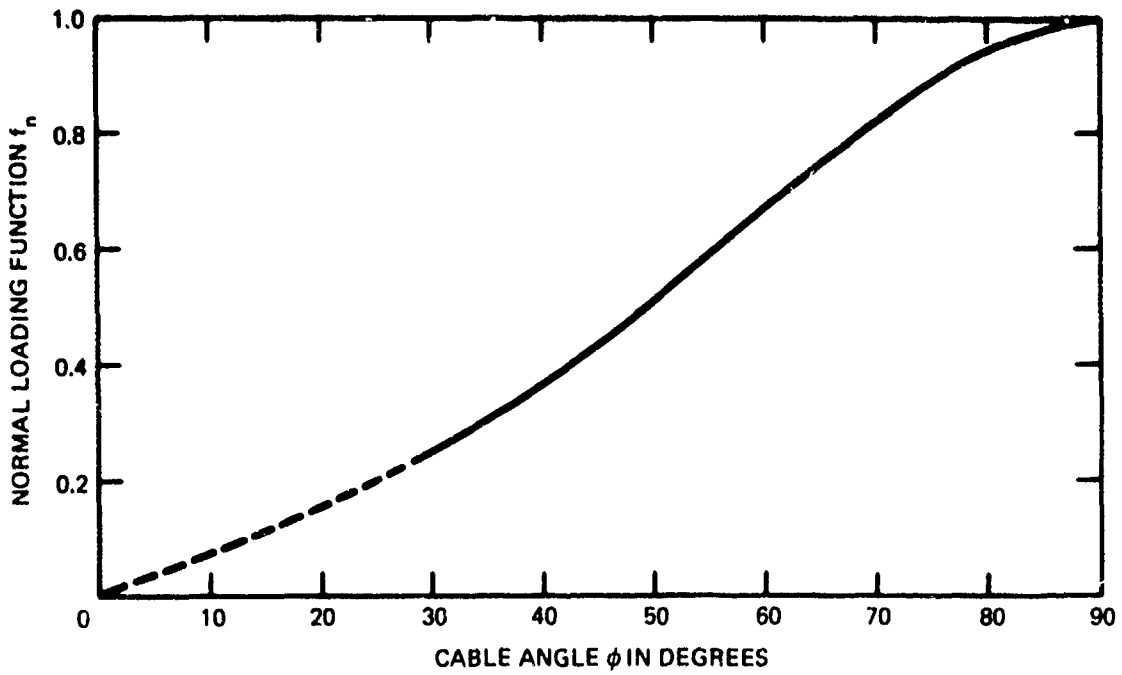


Figure D.15 – Normal Loading Function f_n versus Cable Angle for Model H

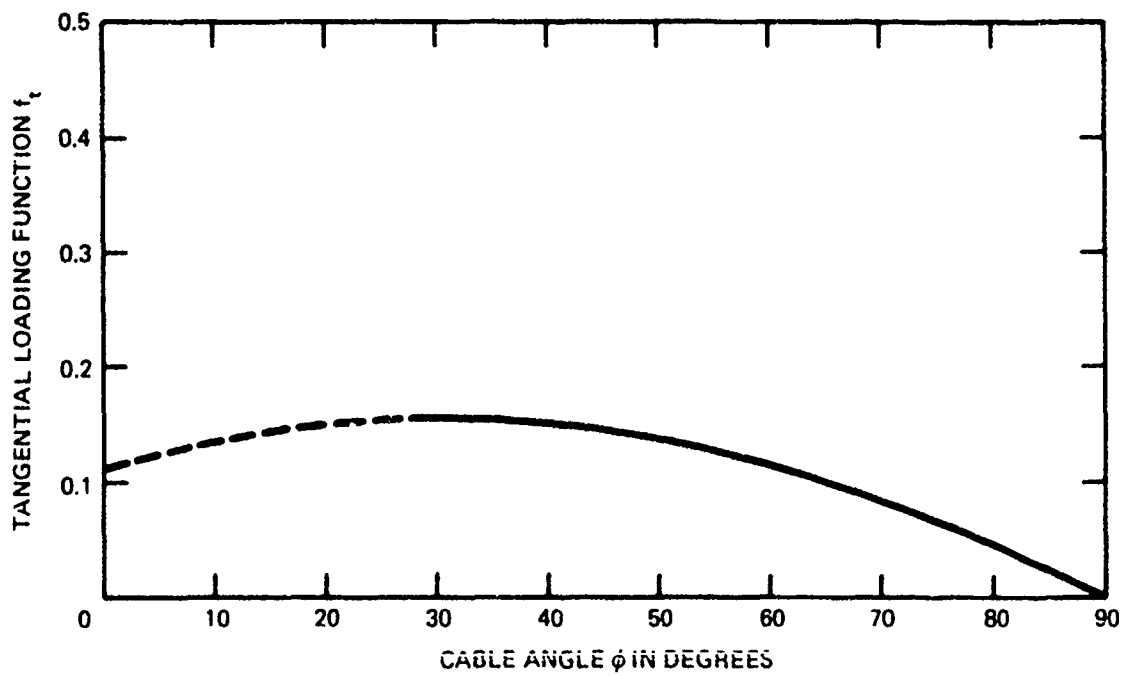


Figure D.16 – Tangential Loading Function f_t versus Cable Angle for Model H

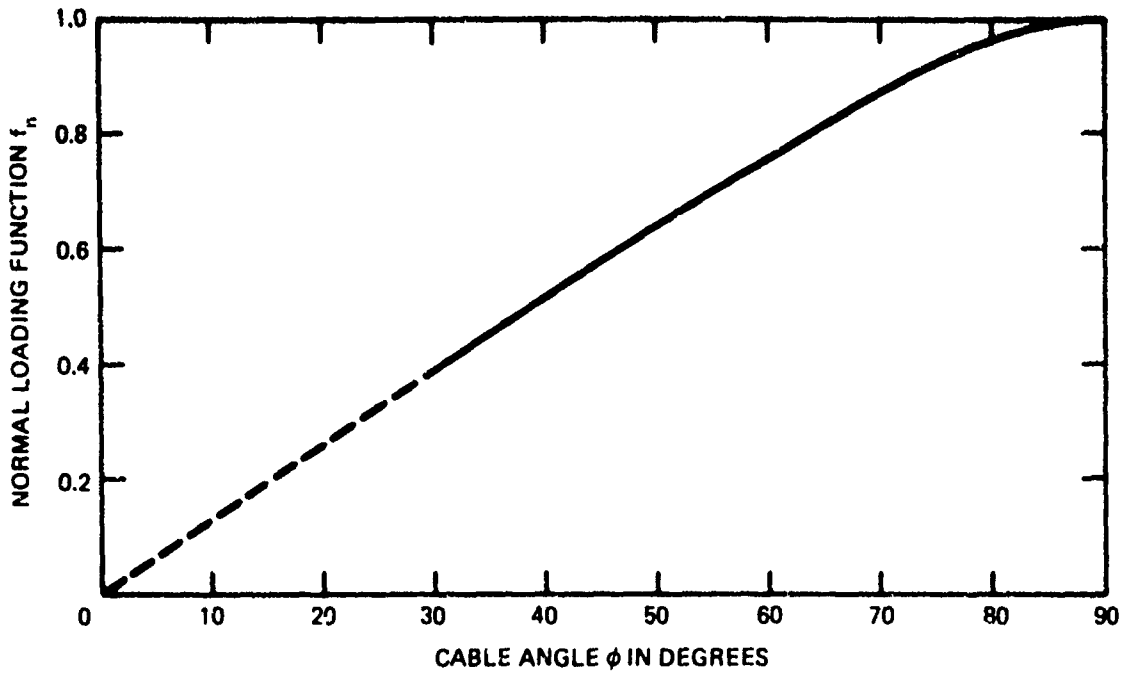


Figure D.17 – Normal Loading Function f_n versus Cable Angle for Model I

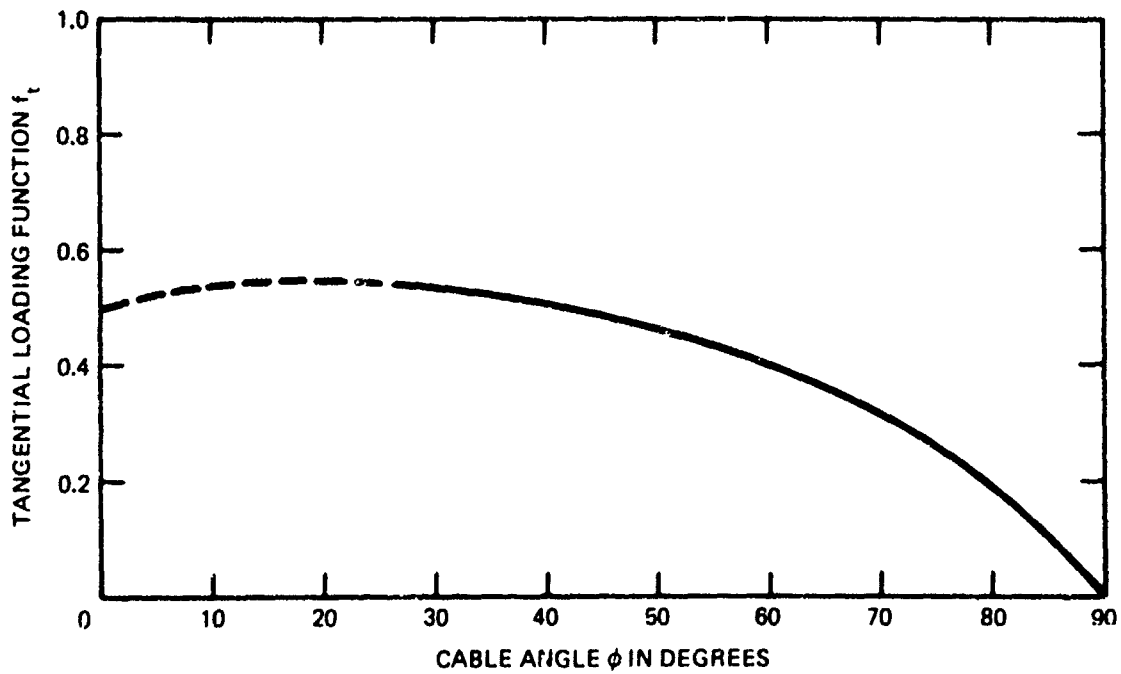


Figure D.18 – Tangential Loading Function f_t versus Cable Angle for Model I

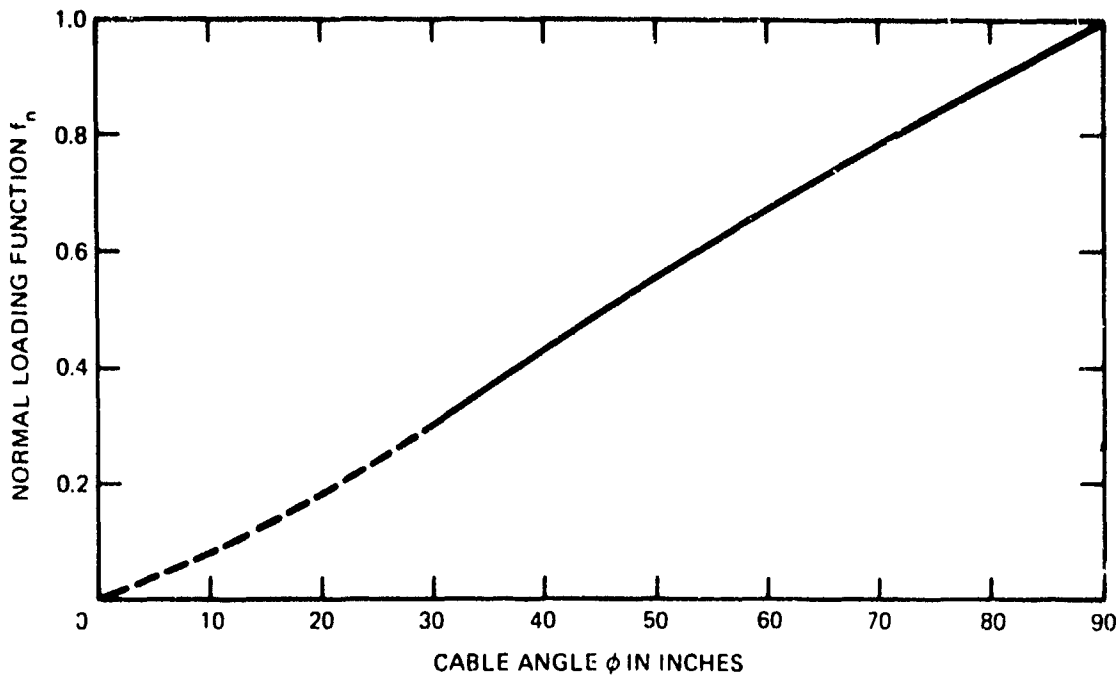


Figure D.19 – Normal Loading Function f_n versus Cable Angle for Model J

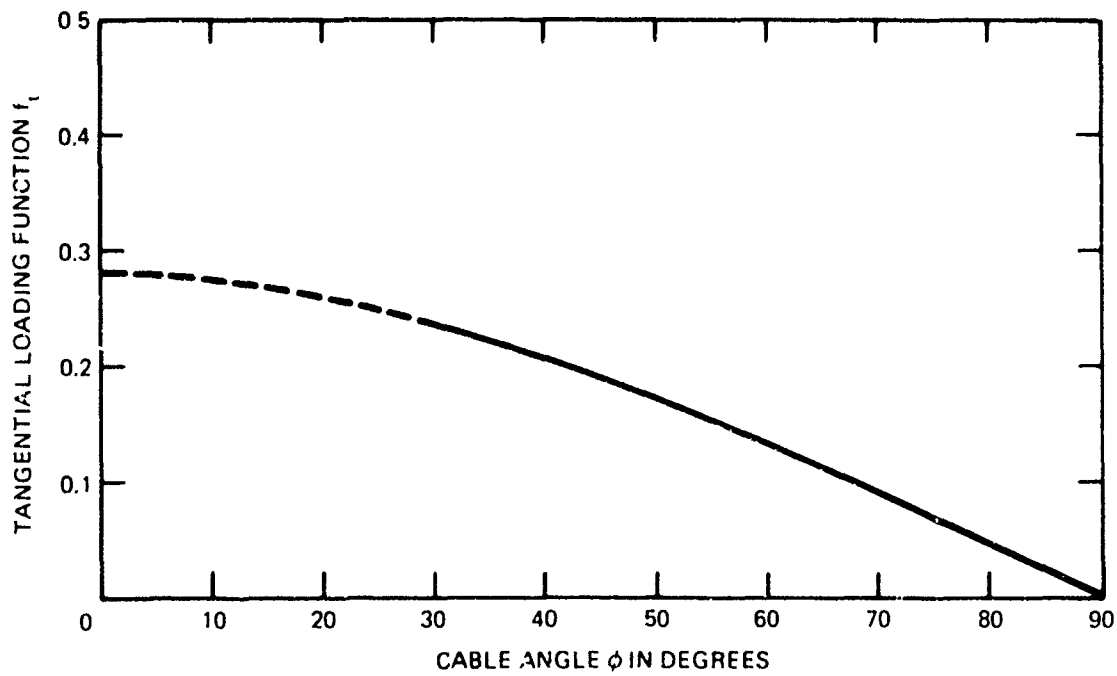


Figure D.20 – Tangential Loading Function f_t versus Cable Angle for Model J

APPENDIX E
GRAPHS OF DRAG COEFFICIENTS

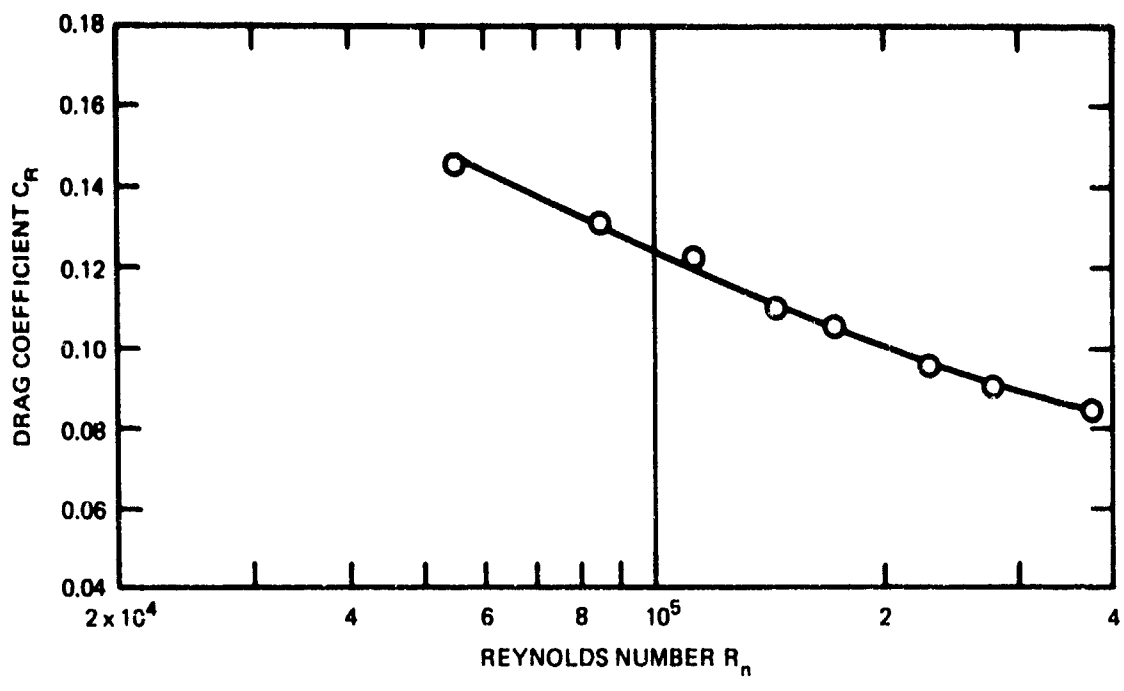


Figure E.1 – Drag Coefficient versus Reynolds Number for Model A

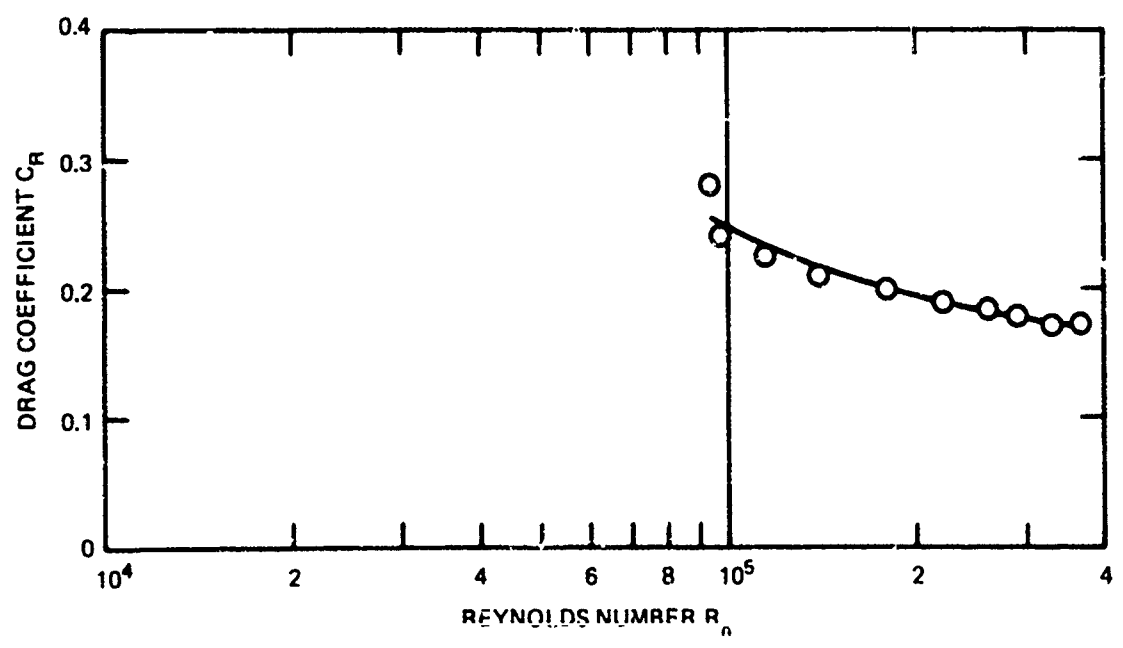


Figure E.2 – Drag Coefficient versus Reynolds Number for Model B

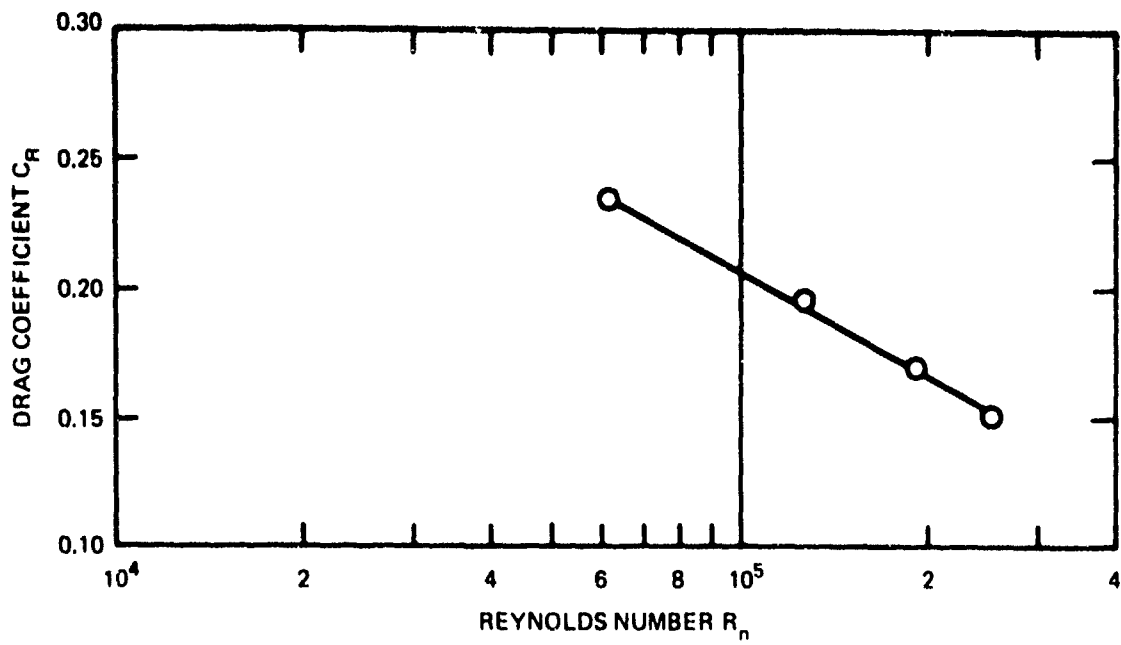


Figure E.3 – Drag Coefficient versus Reynolds Number for Model C

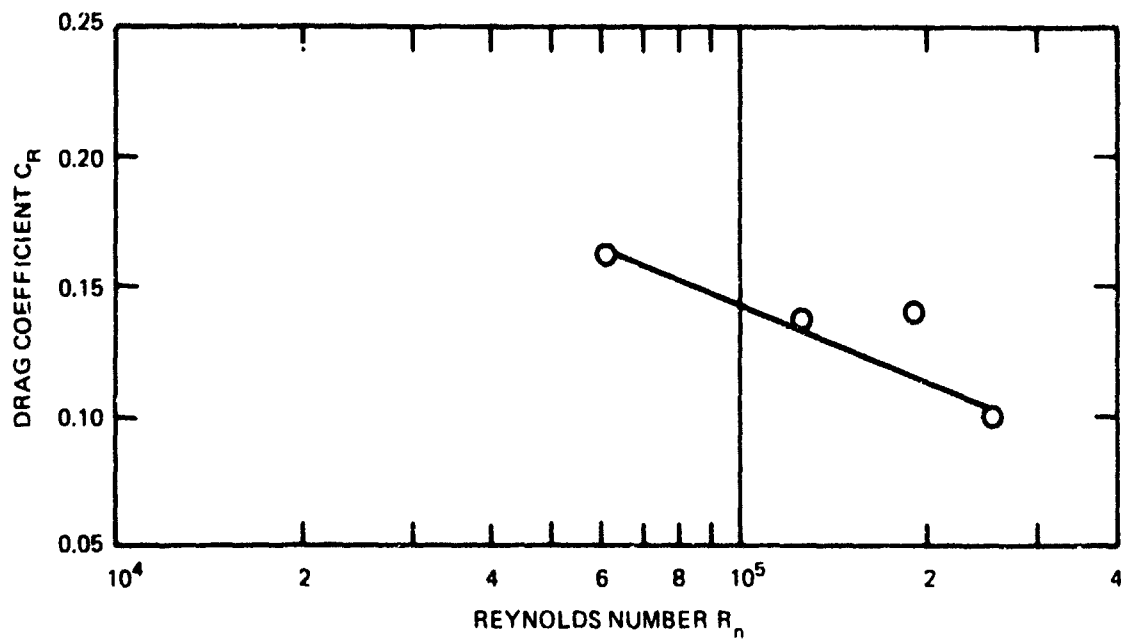


Figure E.4 – Drag Coefficient versus Reynolds Number for Model D

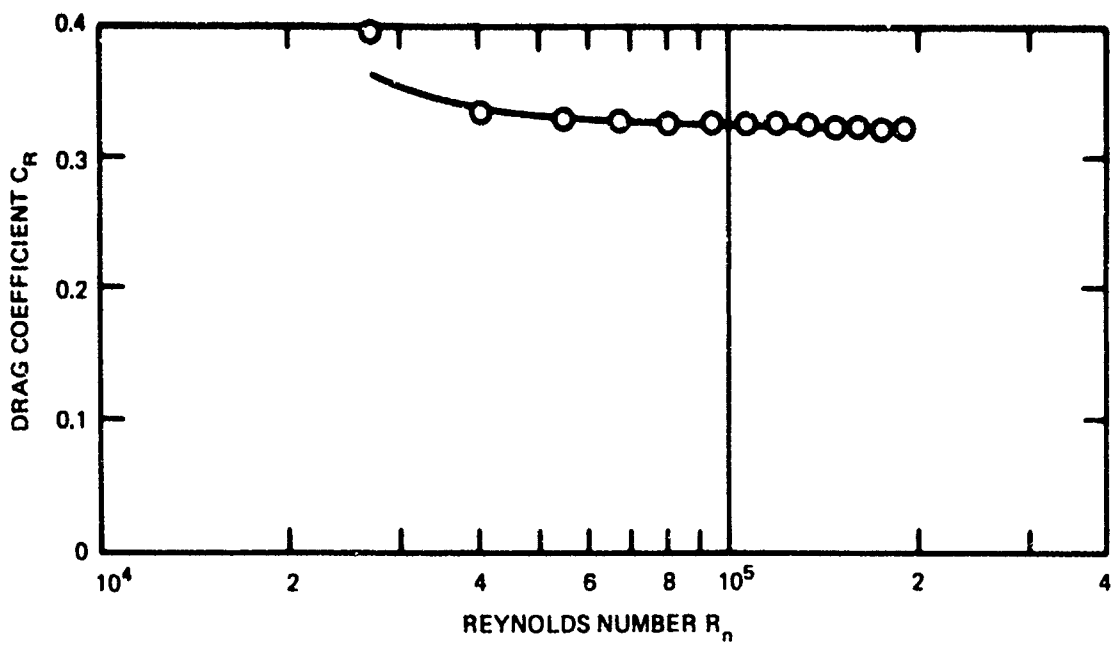


Figure E.5 – Drag Coefficient versus Reynolds Number for Model E

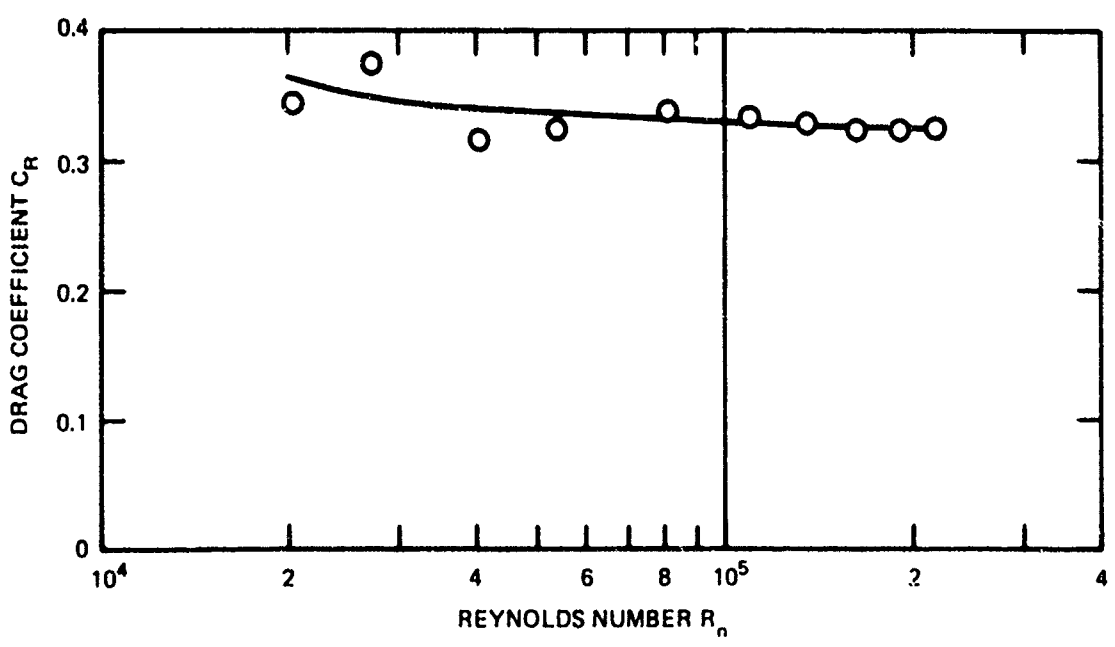


Figure E.6 – Drag Coefficient versus Reynolds Number for Model F

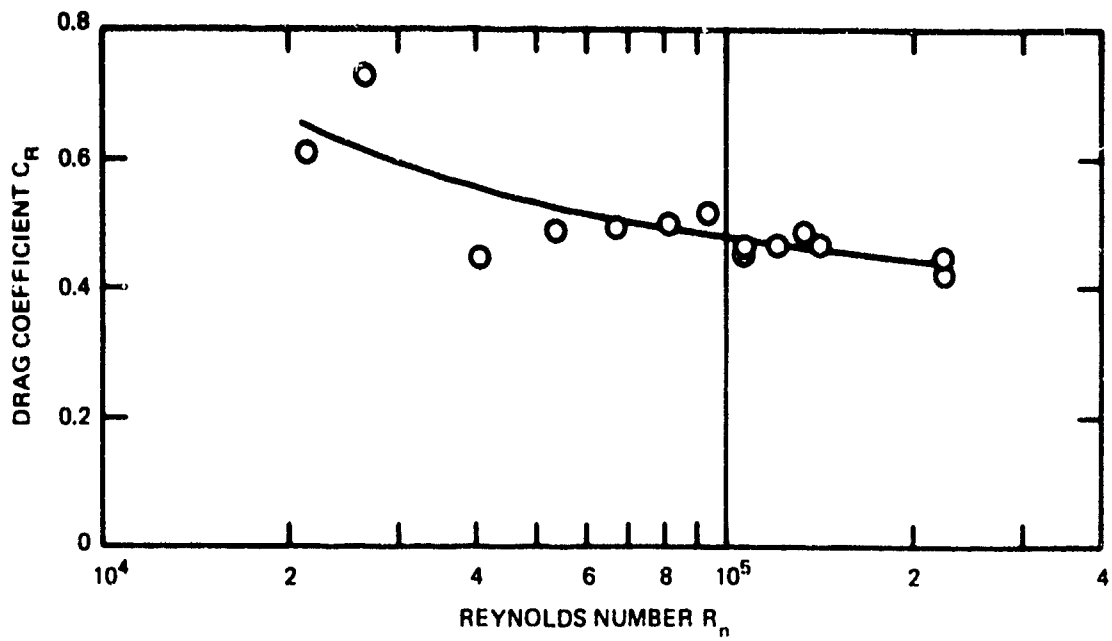


Figure E.7 – Drag Coefficient versus Reynolds Number for Model G

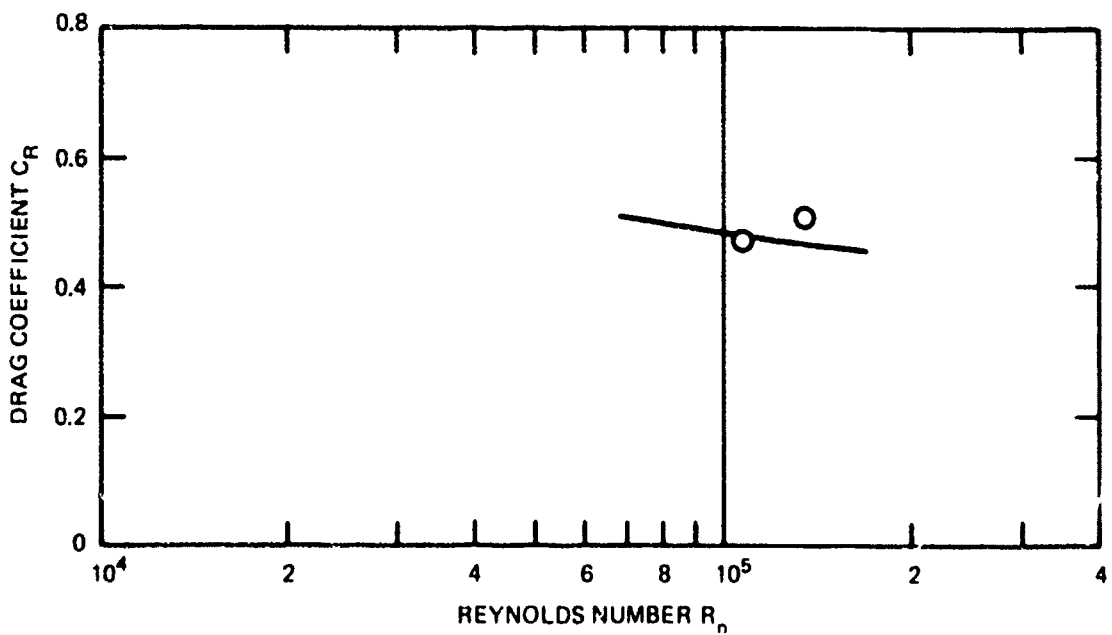


Figure E.8 – Drag Coefficient versus Reynolds Number for Model H

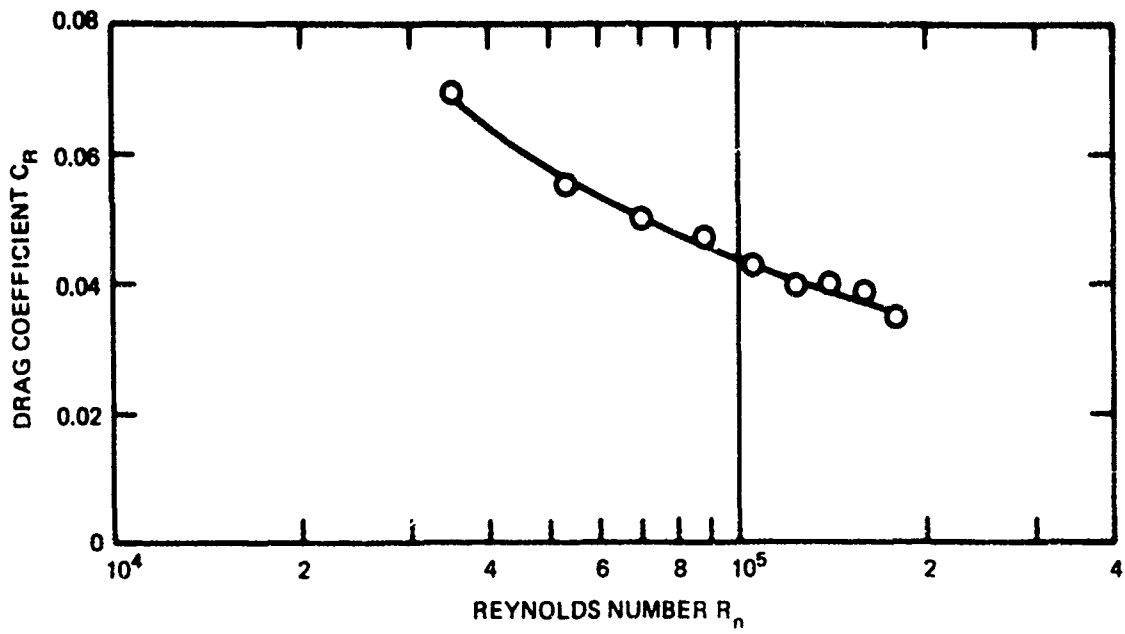


Figure E.9 – Drag Coefficient versus Reynolds Number for Model I

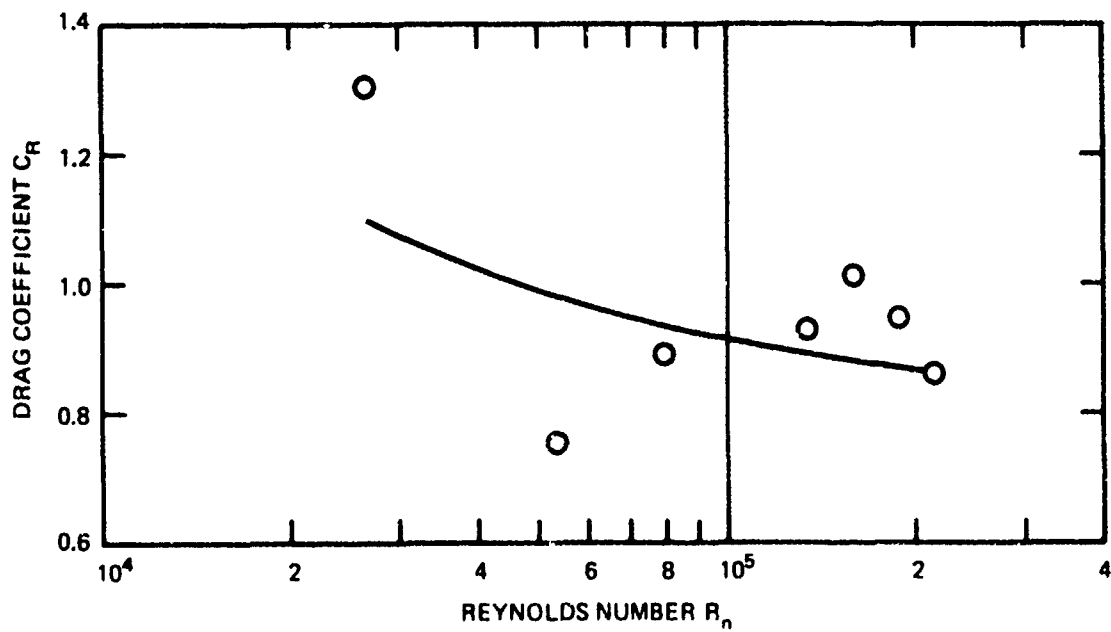


Figure E.10 – Drag Coefficient versus Reynolds Number for Model J

REFERENCES

1. Pode, L., "Tables for Computing the Equilibrium Configuration of a Flexible Cable in a Uniform Stream," David Taylor Model Basin Report 687 (Mar 1951).
2. Cuthill, E.H., "A FORTRAN IV Program for the Calculation of the Equilibrium Configuration of a Flexible Cable in a Uniform Stream," NSRDC Report 2531 (Feb 1958).
3. Whicker, L.F., "The Oscillatory Motion of Cable-Towed Bodies," University of California Report Series No. 82, Issue No. 2 (May 1957).
4. Landweber, L. and M.H. Protter, "The Shape and Tension of a Light, Flexible Cable in a Uniform Current," David Taylor Model Basin Report 533 (Oct 1944).
5. Eames, M.C., "Steady-State Theory of Towing Cables," Defence Research Establishment Atlantic Report 67/5 (1967).
6. Feihner, L.F. and L. Pode, "The Development of a Fairing for Tow Cables," David Taylor Model Basin Report C-433 (Jan 1952) UNCLASSIFIED.
7. Gertler, M., "The DTMB Planar-Motion-Mechanism System," David Taylor Model Basin Report 2523 (Jul 1967).
8. Springston, G.B., "Generalized Hydrodynamic Loading Functions for Bare and Faired Cables in Two-Dimensional Steady-State Cable Configurations," NSRDC Report 2424 (Jun 1967).